nature medicine

Article

https://doi.org/10.1038/s41591-023-02556-5

Selection of cross-reactive T cells by commensal and food-derived yeasts drives cytotoxic T_H1 cell responses in Crohn's disease

Received: 8 March 2023

Accepted: 22 August 2023

Published online: 25 September 2023

Check for updates

Gabriela Rios Martini[1,2], Ekaterina Tikhonova[1,2], Elisa Rosati[1,2], Meghan Bialt DeCelie[3,4,5], Laura Katharina Sievers[2,6], Florian Tran[2,6], Matthias Lessing[6], Arne Bergfeld[6], Sophia Hinz[2,6], Susanna Nikolaus[6], Julia Kümpers[6], Anna Matysiak[6], Philipp Hofmann[1,2], Carina Saggau[1], Stephan Schneiders[1,2], Ann-Kristin Kamps[1,2], Gunnar Jacobs[7], Wolfgang Lieb[7], Jochen Maul[8,9], Britta Siegmund[9], Barbara Seegers[10], Holger Hinrichsen[10], Hans-Heinrich Oberg[1], Daniela Wesch[1], Stefan Bereswill[11], Markus M. Heimesaat[11], Jan Rupp[12], Olaf Kniemeyer[13], Axel A. Brakhage[13,14], Sascha Brunke[15], Bernhard Hube[14,15], Konrad Aden[2,6], Andre Franke[2], Iliyan D. Iliev[3,4,5], Alexander Scheffold[1], Stefan Schreiber[2,6] & Petra Bacher[1,2] ✉

Aberrant $CD4^+$ T cell reactivity against intestinal microorganisms is considered to drive mucosal inflammation in inflammatory bowel diseases. The disease-relevant microbial species and the corresponding microorganism-specific, pathogenic T cell phenotypes remain largely unknown. In the present study, we identified common gut commensal and food-derived yeasts, as direct activators of altered $CD4^+$ T cell reactions in patients with Crohn's disease (CD). Yeast-responsive $CD4^+$ T cells in CD display a cytotoxic T helper cell (T_H1 cell) phenotype and show selective expansion of T cell clones that are highly cross-reactive to several commensal, as well as food-derived, fungal species. This indicates cross-reactive T cell selection by repeated encounter with conserved fungal antigens in the context of chronic intestinal disease. Our results highlighted a role of yeasts as drivers of aberrant $CD4^+$ T cell reactivity in patients with CD and suggest that both gut-resident fungal commensals and daily dietary intake of yeasts might contribute to chronic activation of inflammatory $CD4^+$ T cell responses in patients with CD.

Inflammatory bowel diseases (IBDs) are chronic inflammatory disorders of the gastrointestinal tract, the main forms of which are CD and ulcerative colitis (UC). Control of the immune process through conventional or targeted therapies is poor in these chronic diseases, which results in lifelong morbidity, strongly reduced quality of life and high medical costs. Aberrant immune reactions, particularly $CD4^+$ T cell responses, against members of the intestinal microbiota are considered a causal or driving factor for an IBD. However, the high diversity of the

A full list of affiliations appears at the end of the paper. ✉e-mail: p.bacher@ikmb.uni-kiel.de

microbiome has largely prevented identification of disease-driving, microbial T cell targets and the corresponding microorganism-specific, pathogenic T cell phenotypes in IBDs. Furthermore, owing to the complexity of IBDs, pathogenic CD4$^+$ T cell phenotypes and disease-relevant antigens may also vary for different patient subgroups.

T_H17 cells are regarded as central orchestrators of homeostatic immune responses against microorganisms. Dysregulated T_H17 cell responses, in turn, are thought to contribute to intestinal inflammation and increased levels of interleukin (IL)-17A-producing cells can be found in the intestinal mucosa of patients with IBD[1,2]. However, neutralization of IL-17 has been clinically ineffective in CD and even caused exacerbation in some patients[3,4], suggesting that IL-17A could play a protective rather than a pathological role in CD or in a subgroup of these patients. In this regard, T_H17 cell plasticity and the development of pathogenic T_H17 cell subsets that coexpress inflammatory cytokines, such as interferon (IFN)-γ or granulocyte–macrophage colony-stimulating factor (GM-CSF), might be important determinants for a protective versus a pathogenic role for T_H17 cells[5]. In addition, T_H1 cells expressing the signature cytokine IFN-γ are consistently found to be increased in the intestine of patients with CD, but not those with UC[6]. Thus, deciphering the disease-relevant microbial antigens and unique features of pathogenic, microorganism-specific, CD4$^+$ T cell responses could give rise to the development of targeted therapies.

Most studies to date have addressed alterations in the intestinal bacterial microbiota in IBDs and few studies have analyzed bacteria-specific CD4$^+$ T cell responses[7–14]. Although bacteria are more abundant organisms in the gastrointestinal tract, fungi are an integral, but largely neglected, part of the human intestinal microbiota. Only recently has the important role of individual fungal species on human health and immunopathology come into focus[15–22]. In particular, the intestinal commensal fungus *Candida albicans* has been identified as a major modulator of the human immune system by inducing homeostatic T_H17 cell responses[15,23], as well as intestinal immunoglobulin (Ig)A[17,22] and systemic IgG antibodies[16]. It is still unclear whether *C. albicans*-specific T_H17 cells contribute to intestinal inflammation in patients with IBD or are recruited to the site of inflammation to foster healing. Most interestingly, a high prevalence of anti-*Saccharomyces cerevisiae* antibodies (ASCAs) has been consistently reported in the serum of patients with CD. Although *S. cerevisiae* mannans were usually used as a binding antigen in these assays, further studies have demonstrated that ASCAs also bind to mannans from other fungi, including *C. albicans*[24]. In addition to *C. albicans*, the human intestine also harbors a plethora of other commensal, as well as food-derived, fungi[25–27]. Whether these fungal species can also actively modulate human immune responses has not yet been addressed.

In the present study, we show that CD4$^+$ T cell responses against commensal and food-derived yeasts are strongly increased in blood and inflamed tissue of patients with CD, but not those with UC. These yeast-reactive CD4$^+$ T cells display cytotoxic T_H1 cell effector functions, whereas *C. albicans*-specific T_H17 cell responses remain largely unchanged. Cytotoxic T_H1 cells are clonally expanded and highly cross-reactive to several commensal and food-derived yeast species, indicating their selection by chronic encounter with conserved antigens that are present in different yeasts. Our data identify commensal and dietary yeasts as drivers of aberrant CD4$^+$ T cell reactivity in patients with CD and suggest that repeated encounter with conserved antigens present in different microbial species may lead to the expansion and chronic activation of cross-reactive, yeast-responsive, CD4$^+$ T cells. This could reveal a general mechanism of how selection of cross-reactive T cells may allow adaptive immunity to cope with the enormous diversity of microbial antigens which, if not properly regulated, could come at the expense of fostering chronicity and contribution to therapy resistance in IBD due to persistent antigen activation.

Results

CD4$^+$ T cell responses against yeasts are increased in CD

To identify microbial species driving pathogenic T cell responses in IBDs, we analyzed the CD4$^+$ T cell reaction against common bacterial and fungal species of the human intestinal microbiome in patients with IBD and healthy donors (see Extended Data Tables 1 and 2 for demographic data). Peripheral blood mononuclear cells (PBMCs) were stimulated ex vivo for 7 h with whole bacterial and fungal lysates. The differentially stimulated cells were labeled with CD4 antibody-based fluorescent barcodes, allowing multiplexed analysis of T cell reactivity against different species (Extended Data Fig. 1a). Microorganism-reactive CD4$^+$ T cells were detected based on magnetic enrichment of CD154 (CD40L)-expressing cells (antigen-reactive T cell enrichment (ARTE))[15,28] (Extended Data Fig. 1a,b). Specificity of CD154$^+$ induction by microbial lysates was confirmed by blocking antigen presentation with a human leukocyte antigen (HLA)-DR antibody (Extended Data Fig. 2a–c) and by restimulation of expanded CD154$^+$ T cells with specific or unrelated antigen lysates (Extended Data Fig. 2d).

Circulating CD45RA$^-$ memory T cells (T_{mem} cells) reactive against different microbial species were detected with variable frequencies (range 0.0001–0.76%) (Fig. 1a,b). Although *C. albicans*, the most abundant intestinal fungal commensal[20,29] (Fig. 1c), elicited the strongest reactivity in healthy individuals, we observed only a slight increase in reactive T_{mem} cells in patients with CD. In sharp contrast, reactivity against other less abundant *Candida* spp., as well as against the food-associated yeast *Saccharomyces cerevisiae* (Fig. 1c), was dramatically elevated in patients with CD, but not those with UC (Fig. 1a,b). No significant differences were observed against the phylogenetically distant yeast *Malassezia restricta* or the analyzed bacterial species (Fig. 1a,b). Together this indicates an altered antifungal immune response to gut mycobiota in patients with CD. However, we also

Fig. 1 | Altered CD4$^+$ T cell reactivity against fungal microorganisms in CD patients. a, Frequencies of reactive CD154$^+$CD45RA$^-$CD4$^+$ T_{mem} cells against whole microbial lysates in healthy donors and patients with an IBD: healthy donors (HD, black dots), CD (red dots) and UC (gray dots). The letter *n* indicates the number of individual donors specified below each group. The *P* values are given at the top of each figure. **b**, Dot plot examples for the ex vivo detection of microorganism-reactive CD4$^+$ T cells by ARTE. Absolute cell counts after magnetic CD154$^+$ enrichment from 1×10^7 PBMCs are indicated. w/o, without. **c**, ITS-seq and analysis of stool samples from patients with CD ($n = 38$). The relative abundance of the top 12 fungal species identified by this analysis is shown. Less abundant or less represented fungal species are grouped under 'other'. **d**, Serum anti-IgG and IgA ASCA concentrations in healthy donors and patients with IBD (HD, $n = 46$; CD, $n = 88$; UC, $n = 73$). Sera were considered positive if their activity was >20 relative units (RU) per ml. Both single-positive IgA or IgG samples and double-positive samples classified donors who are ASCA$^+$. **e**, Frequencies of fungus-reactive CD4$^+$ T cells in patients with CD, according to their ASCA status. **f**, Total CD4$^+$ T_{mem} cells isolated from biopsies of inflamed and uninflamed intestinal tissue of patients with CD who are ASCA$^+$ ($n = 5$). Cells were seeded at 200 cells per well in multiple wells, and expanded and restimulated with fungal lysates in the presence of autologous APCs. Mean frequencies of reactive CD154$^+$ cells for all wells per patient are shown. **g**, Dot plot examples for restimulation of expanded CD4$^+$ T_{mem} cells from an inflamed biopsy. The percentage of CD154$^+$ TNF$^+$ cells within CD4$^+$ is indicated. Each symbol in **a**, **d**, **e** and **f** represents one individual donor and horizontal lines in **a** and **e** indicate the mean. Box-and-whisker plots are shown in **c** with center lines representing the median, box limits 25% (lower) and 75% (upper) quartiles and whiskers the minimum/maximum. Truncated violin plots with quartiles and range are shown in **f**. Statistical differences were obtained using the Kruskal–Wallis test with Dunn's post hoc test in **a** with only significant differences shown; the two-tailed Mann–Whitney *U*-test was used in **e**.

https://doi.org/10.1038/s41591-023-02556-5

noticed a high heterogeneity in the frequencies of antifungal T cells between different patients with CD (Fig. 1a). ASCAs can be detected in the serum of 50–60% of patients with CD and are used as a biomarker of disease severity[30]. When stratifying our cohort of patients with CD according to their ASCA immunoglobulin IgG/IgA status (Fig. 1d), strikingly, increased yeast-reactive T cell responses were detected

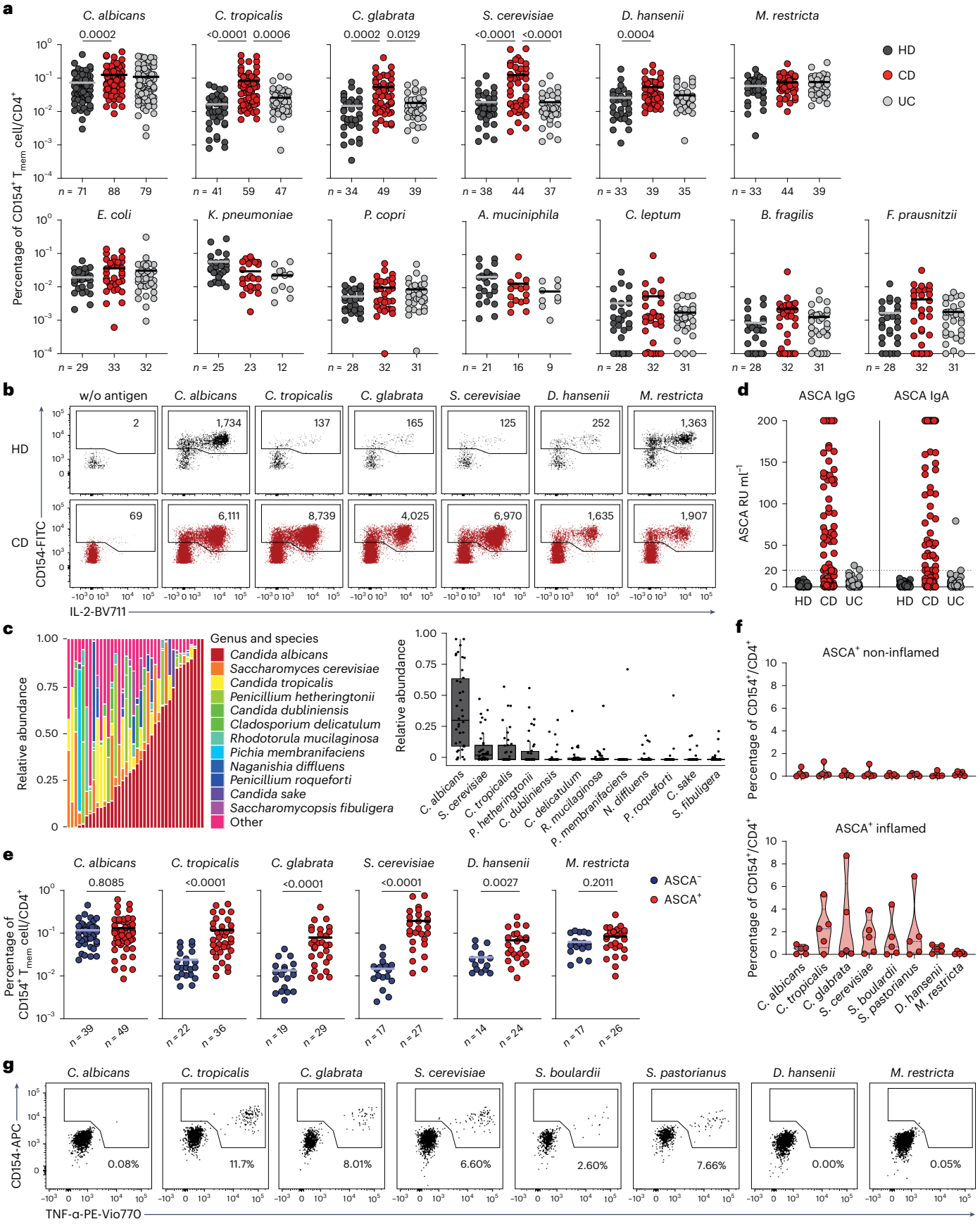

https://doi.org/10.1038/s41591-023-02556-5

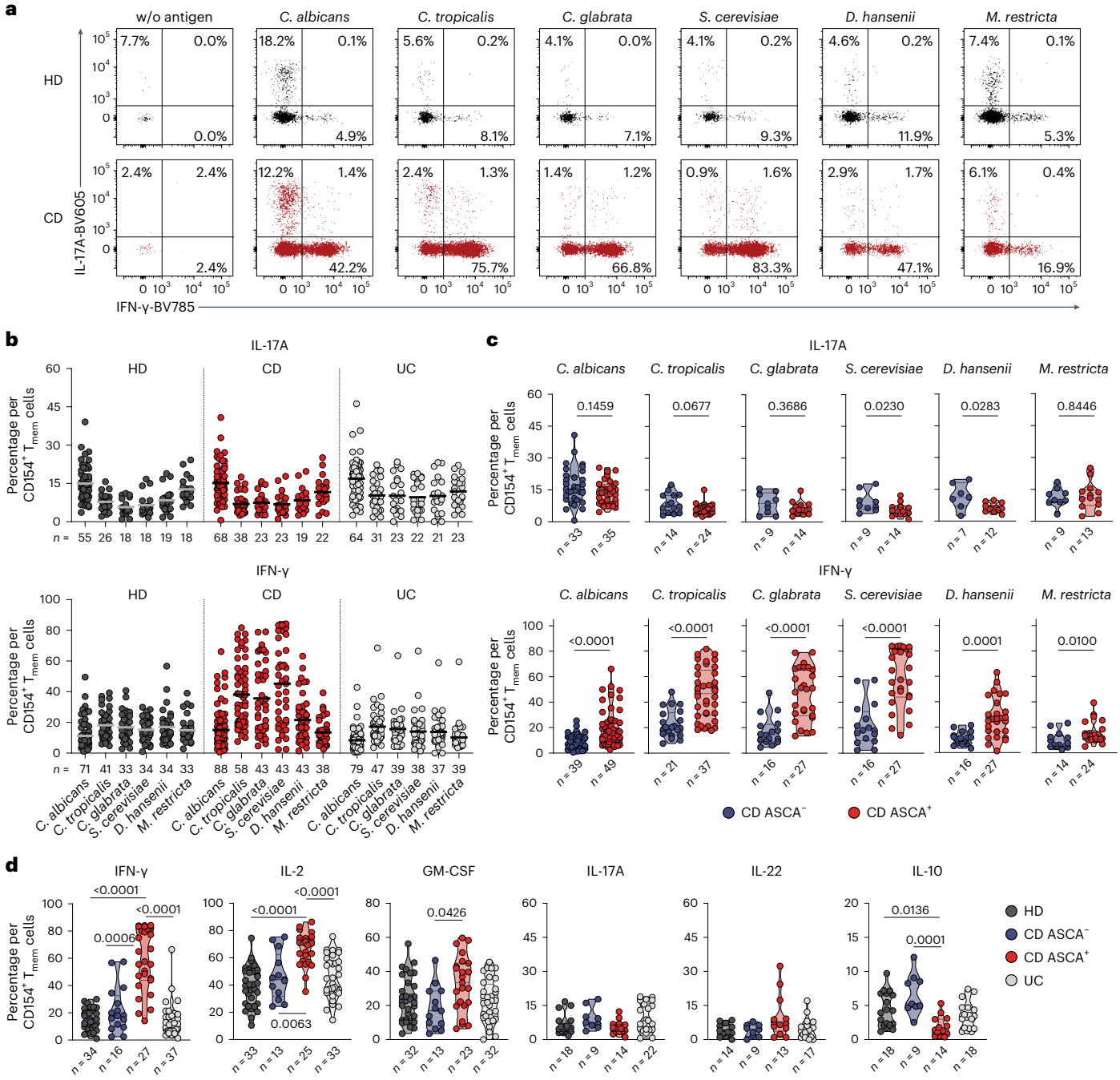

Fig. 2 | Enhanced T_H1 cell but not T_H17 cell responses against yeasts in patients with CD. a,**b**, Ex vivo cytokine production of fungus-reactive T_{mem} cells following ARTE. **a**, IL-17A and IFN-γ staining of yeast-reactive CD154$^+$ T cells. **b**, Statistical summary in healthy donors and patients with IBD. **c**, IL-17A and IFN-γ production of yeast-reactive CD4$^+$ T cells in patients with CD according to their ASCA status. **d**, Cytokine production of *S. cerevisiae*-reactive T cells in healthy donors and patients with IBD. Each symbol in **b**, **c** and **d** represents one individual donor and horizontal lines indicate the mean. Truncated violin plots with quartiles and range are shown in **c** and **d**. Statistical differences (shown in figures) were obtained using the two-tailed Mann–Whitney *U*-test in **c** and the Kruskal–Wallis test with Dunn's post hoc test in **d**; only significant differences are shown.

in ASCA$^+$, but not ASCA$^-$, patients with CD (Fig. 1e). In contrast, the strong T_{mem} cell response to *C. albicans* was independent of the ASCA status.

These results indicate that, in addition to augmented T_{mem} cell responses to commensal *C. albicans* in patients with CD[15], a cohort of ASCA$^+$ patients develops unexpected T cell reactivity to less represented fungal commensals and food-derived yeast species that so far have not been described as major inducers of T cell reactivity in humans.

Yeast-reactive CD4$^+$ T cells are enriched in inflamed mucosa

We next analyzed whether yeast-responsive T cells are also present at the site of intestinal inflammation. As the cell numbers obtained from intestinal biopsies are too low for direct analysis by ARTE, we expanded total CD4$^+$ T cells from inflamed and noninflamed gut biopsies polyclonally and restimulated them with various fungal lysates. Yeast-reactive T cells were selectively present in inflamed gut tissue from patients who were ASCA$^+$, but not in noninflamed tissue from the same individuals (Fig. 1f,g), or in tissue from patients with CD

who are ASCA$^-$ (Extended Data Fig. 2e). Notably, this applied also to other *Saccharomyces* spp., such as *Saccharomyces pastorianus* or the probiotic yeast *Saccharomyces boulardii*, which is sometimes used as a treatment supplement for IBD[31], whereas reactivity to *C. albicans* was low (Fig. 1f). We further examined whether the increased T cell reactivity against yeasts might be influenced by disease state or duration. There were no significant correlations of yeast-reactive T cell frequencies with disease duration, medication or activity, as determined by the Harvey–Bradshaw index and the CD activity index (Extended Data Fig. 3).

In summary, these data reveal an unexpected increase of CD4$^+$ T cell reactivity against intestinal commensal and food-derived yeasts in blood and inflamed tissue in patients with CD who are ASCA$^+$. Although *C. albicans* dominates the antifungal T cell response in healthy individuals and *C. albicans*-reactive T cells are still highly present in patients with CD, the increased T cell reactivity in patients with CD who are ASCA$^+$ was mainly directed against non-*albicans Candida* spp., as well as food-associated *Saccharomyces* spp.

Yeast-reactive CD4$^+$ T cells show increased IFN-γ production

Intestinal inflammation in IBD has been linked to aberrant T_H17 cell responses and the development of pathogenic T_H17 cells which coproduce inflammatory cytokines such as IFN-γ[1,2]. We recently showed that, within a number of species found in the human mycobiome, *C. albicans* is the major driver of fungus-reactive T_H17 cells in humans[15]. However, we detected no significant differences of fungus-reactive IL-17A production in patients with IBD compared with healthy donors (Fig. 2a,b). In contrast, CD4$^+$ T cells reactive against the different yeast species, including *C. albicans*, showed a massively increased IFN-γ production in patients with CD (Fig. 2a,b), which was again strongly enhanced in individuals who are ASCA$^+$ compared with those who are ASCA$^-$ (Fig. 2c). Just as for the frequencies (Fig. 1), the increased IFN-γ production was much more pronounced for non-*albicans Candida* spp. and especially for *S. cerevisiae*. We observed only low coexpression of IFN-γ and IL-17A (Fig. 2a), indicating selective T_H1 cell expansion rather than T_H1 cell-like modulation of pre-existing T_H17 cells. However, small populations (≤5%) of IL-17A$^+$IFN-γ$^+$ coproducing cells were also increased against *Candida* spp. and *S. cerevisiae* (Extended Data Fig. 4a,b). Further characterization of yeast-reactive T cells revealed enhanced production of several inflammatory cytokines in response to *S. cerevisiae* and *Candida tropicalis*, including IL-2 and GM-CSF, whereas IL-10 production was significantly reduced in patients with CD who are ASCA$^+$ (Fig. 2d and Extended Data Fig. 4c,d). Again, we observed no differences of *M. restricta*-reactive T cells (Extended Data Fig. 4d).

Collectively, these data show strongly increased inflammatory T_H1 cell responses against *Candida* and *Saccharomyces* yeasts in patients with CD who are ASCA$^+$ and only a minor development of IL-17A$^+$IFN-γ$^+$ cells. In contrast, the proportion of IL-17A producers within *C. albicans*-specific T cells was conserved and remained largely unaffected by the disease.

Yeast-reactive T_H1 cells have a cytotoxic signature

To obtain deeper insights into the cellular composition of yeast-reactive T cells and their functional capacities, we performed single-cell RNA sequencing (scRNA-seq) of ex vivo FACS-purified, *C. albicans*-, *C. tropicalis*- and *S. cerevisiae*-reactive CD154$^+$ T_{mem} cells from three patients with CD who are ASCA$^+$ and three healthy donors (Fig. 3a). In total, we sequenced 15,012 *C. albicans*-, 21,623 *C. tropicalis*- and 23,495 *S. cerevisiae*-reactive CD4$^+$ T cells. Within these cells, we identified eight clusters with a distinct transcriptional profile based on Leiden unsupervised clustering (Fig. 3b,c). Among these clusters, we detected again a dominant T_H1 cell population (marker genes *IFNG* and *TBX21)* that was additionally characterized by expressing high levels of cytotoxic marker genes (for example, *PRF1*, *GZMB* and *SLAMF7*) (Fig. 3c). In fact, cells within this cluster expressed a number of genes previously described for cytotoxic CD4$^+$ T cells that arise in viral infections or cancer[32] (Extended Data Fig. 5a,b). Furthermore, these cells expressed high levels of *HOPX*, encoding a transcription factor that has been associated with chronic T cell activation[33,34]. The T_H1 cell-cytotoxic cluster was strongly increased in patients with CD compared with healthy donors (Fig. 3b,d). We also noticed the increase of an effector cluster in *C. tropicalis*- and *S. cerevisiae*-reactive cells from patients with CD expressing low levels of T_H17 cell signature genes (*IL17A* and *IL22*), but also of T_H1 cell marker genes *IFNG* and *TBX21*, as well as *CSF2* and *IL2* (Fig. 3c,d). Discrimination of healthy and patient-derived cells in this cluster revealed that CD-derived cells did not upregulate T_H17 cell genes, but rather several other inflammatory genes defining this cluster (that is, *IFNG*, *TBX21*, *CSF2* and *IL2*) (Extended Data Fig. 5c). This is in line with the low proportion of IL-17A protein-expressing cells (Fig. 2b) and was further confirmed by direct hashtag antibody labeling of IL-17A protein-secreting T cells, which did not increase in patients with CD (Extended Data Fig. 5d,e). The other identified gene clusters either remained unchanged or were reduced in patients with CD versus controls or in general comprised only a small proportion (≤5%) of cells (Fig. 3d).

Development of T_H17 cells into pathogenic IL-17A$^+$IFN-γ$^+$ coproducing cells or even a complete conversion of T_H17 cells into T_H1 cells has been suggested to occur in chronic inflammation[5,34]. Based on intracellular cytokine staining, we observed only a minor proportion of cells coexpressing IFN-γ and IL-17A cytokines (Fig. 2a). To further analyze the developmental origin of the yeast-reactive cytotoxic T_H1 cells (T_H1-CTLs), we next performed a pseudotime analysis, which reveals pseudo-temporal ordering of cells according to gene expression similarity. Using the Monocle algorithm[35], we identified two major trajectories, starting from central memory cells (T_{CM} cells) to either the effector/T_H17 cell cluster or the T_H1-CTL lineage (Fig. 3e). This supports the conclusion that the T_H1-CTLs do not primarily convert from T_H17 cell precursors. It is interesting that expression of *IFNG* and *TBX21* preceded the expression of cytotoxic marker genes along the T_H1-CTL branch, pointing to a progressive acquisition of cytotoxic effector functions in T_H1 cells over time (Fig. 3f).

Together, our data reveal that, in CD, but not under a steady state, exposure to yeast antigens results in strong expansion of yeast-reactive T_H1 cells with a cytotoxic signature.

T_H1-CTLs have killing ability for IECs

We confirmed the protein expression of cytotoxic markers by yeast-reactive CD4$^+$ T_H1 cells in patients with CD by flow cytometry

Fig. 3 | Yeast-reactive CD4$^+$ cells from patients with CD have a cytotoxic phenotype. a, Overview of the experimental design. PBMCs of each of three healthy donors and patients with CD who were ASCA$^+$ were stimulated with *C. albicans*, *C. tropicalis* and *S. cerevisiae* lysates. Reactive CD154$^+$ T_{mem} cells were FACS purified (see Methods for sorting) and analyzed by scRNA- and TCR-seq. **b**, UMAP visualization showing the subset composition of yeast-reactive CD4$^+$ T cells colored by different gene expression clusters. **c**, Dot plot visualization showing the expression of selected marker genes in each T cell cluster. Colors represent the normalized mean expression levels and size indicates the proportion of cells expressing the respective genes (T_{cm} cell, central memory cell; T_{TM} cell, transitional memory cell; T_{EM} cell, effector memory cell; T_{FH}, cell follicular helper cell; T_{FR} cell, follicular regulatory cell). **d**, Proportion of cells within each T cell cluster for individual donors (healthy, $n = 3$; CD, $n = 3$). **e**, Trajectory plot of cells ordered along pseudotime (left) and overlaid with their cluster identity (right). **f**, Heatmap depicting gene expression of cluster-defining genes along the trajectory branches identified in **e**. Each symbol in **d** represents one individual donor, and truncated violin plots with quartiles and range are shown.

https://doi.org/10.1038/s41591-023-02556-5

(Fig. 4a,b). Again, T_H1-CTLs were present in patients with CD who were ASCA$^+$, but not in those who were ASCA$^-$ (Fig. 4c and Extended Data Fig. 5f,g). To further investigate the killing capacity of yeast-reactive T_H1-CTLs, we set up an in vitro cytotoxicity assay (Fig. 4d). CD154$^+$ T_{mem} cells reactive to *S. cerevisiae* or *M. restricta*, used as a control antigen, were ex vivo isolated from healthy individuals and patients with CD

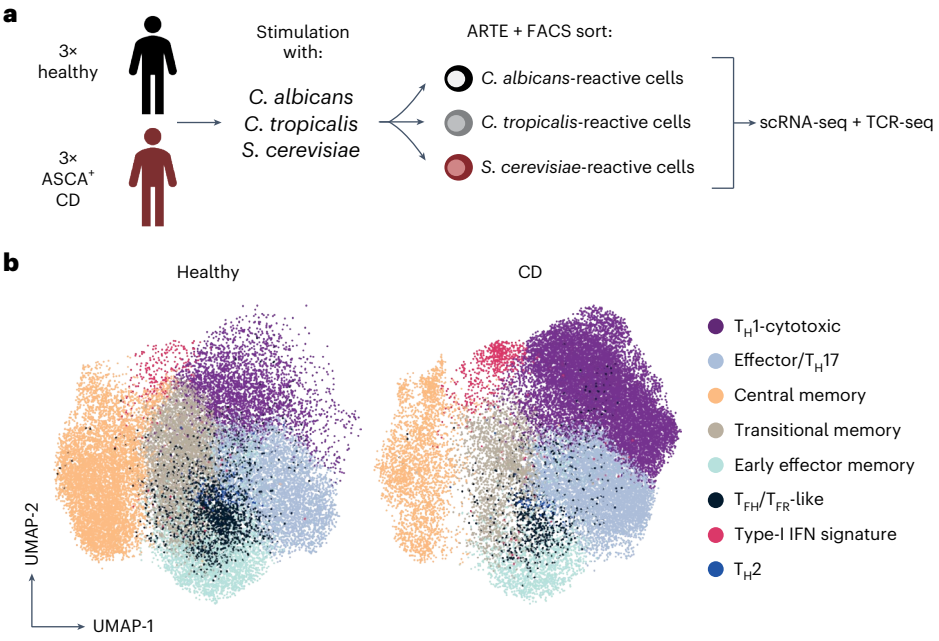

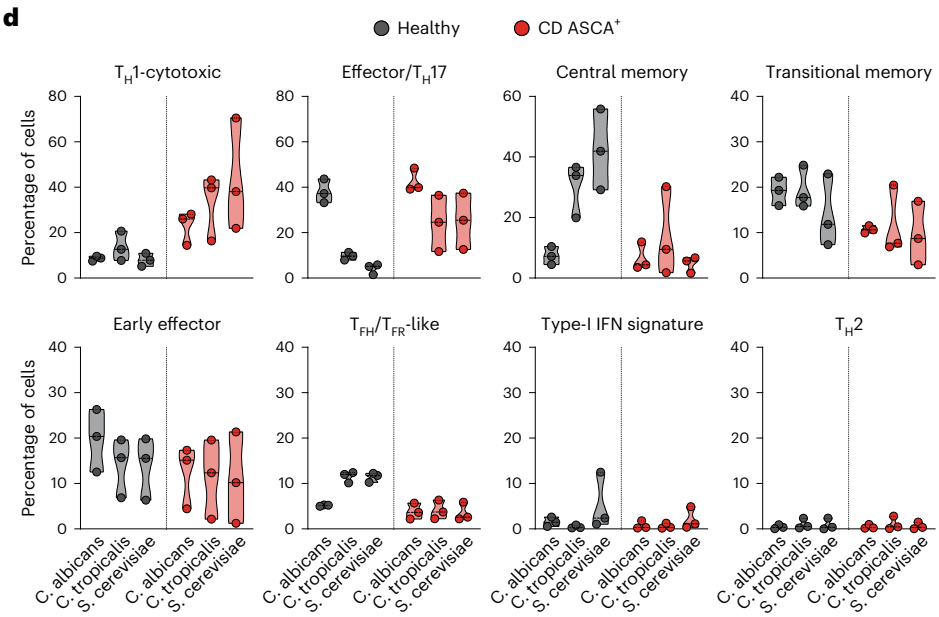

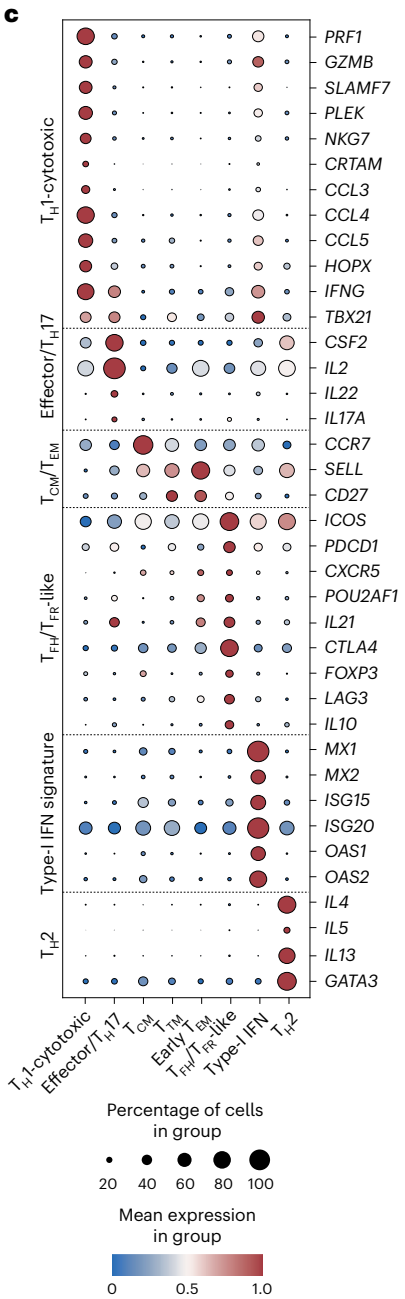

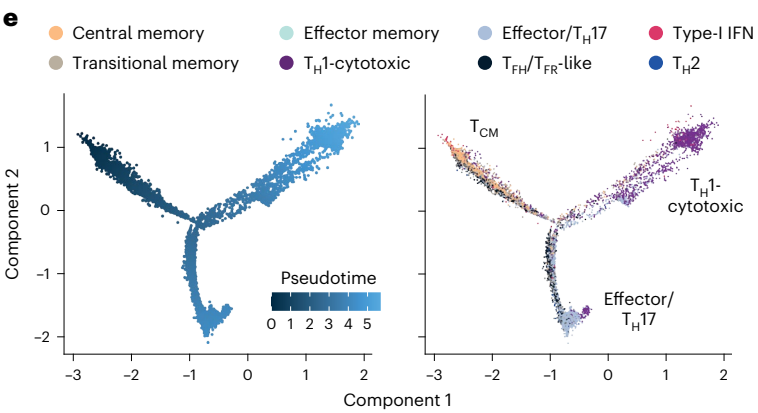

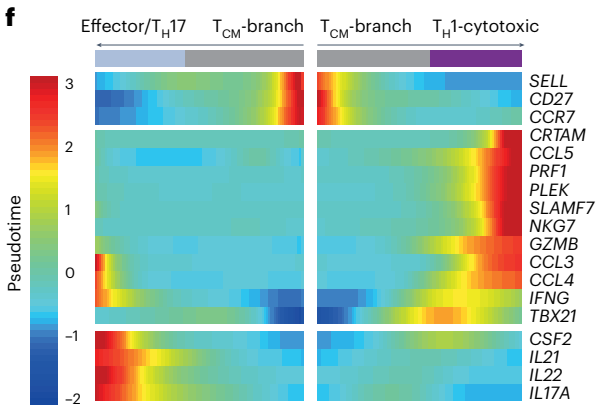

https://doi.org/10.1038/s41591-023-02556-5

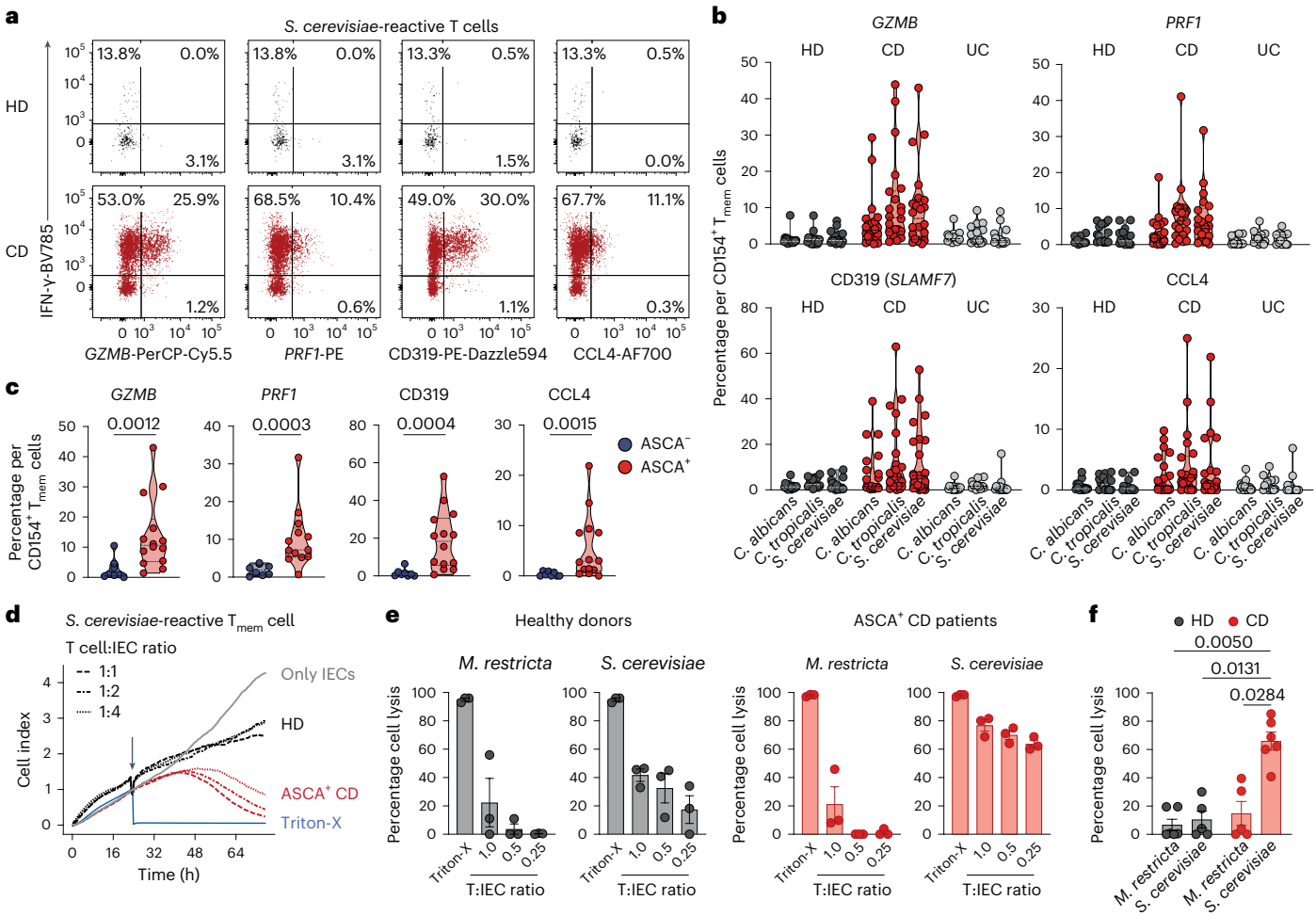

Fig. 4 | Yeast-responsive T_H1-CTLs from patients with CD have potent killing ability for IECs. a, Ex vivo staining of cytotoxic markers (GZMB, PRF1, CD319 and CCL4) and IFN-γ of *S. cerevisiae*-reactive CD154$^+$ T_{mem} cells. **b**, Statistical summary (HD, $n = 16$; CD, $n = 22$; UC, $n = 15$). **c**, Expression of cytotoxic markers in *S. cerevisiae*-reactive T cells of patients with CD according to their ASCA status (ASCA$^-$, $n = 8$; ASCA$^+$, $n = 14$). **d**, Real-time monitoring of cytotoxicity by electrical impedance measurement. Fungus-reactive CD154$^+$ T_{mem} cells were incubated with primary IECs at the indicated T cell-to-target ratios (T:IECs) and IEC killing was monitored via changes in the cell index. Gray line: IECs without added T cells; blue line: IECs after adding the detergent Triton X-100 (positive control for maximal lysis); black lines: T cells from an HD; red lines: T cells from a patient with CD who was ASCA$^+$. **e**, Summary of T cell-mediated killing after 35 h of coculture for *M. restricta*- and *S. cerevisiae*-reactive T_{mem} cells at different T cell-to-IEC ratios (healthy, $n = 3$; ASCA$^+$ CD, $n = 3$). **f**, Statistical summary of T cell-mediated killing at a T cell-to-IEC ratio of 1:4 (HD *S. cerevisiae*, $n = 5$; *M. restricta*, $n = 6$; CD *S. cerevisiae*, $n = 6$, *M. restricta* $n = 5$). Each symbol in **b**, **c**, **e** and **f** represents one donor. Truncated violin plots with quartiles and range are shown in **b** and **c**. Error bars indicate mean and s.e.m. in **e** and **f**. Statistical differences were obtained with the two-tailed Mann–Whitney *U*-test in **c** and the Kruskal–Wallis test with Dunn's post hoc test in **f**. Statistical differences to *S. cerevisiae*-reactive cells from patients with CD are indicated.

who were ASCA$^+$ and cocultured with allogeneic primary intestinal epithelial cells (IECs) in different ratios. T cells and IECs were cross-linked by the addition of *Staphylococcus* enterotoxin B (SEB) and the killing of the IECs was measured by real-time cell analysis. In line with their cytotoxic signature, *S. cerevisiae*-reactive CD4$^+$ T cells from patients with CD who were ASCA$^+$, but not from healthy donors, lysed IECs in a dose-dependent manner. No cytotoxicity was observed when *M. restricta*-reactive CD4$^+$ T cells were used (Fig. 4e,f).

These data confirm that yeast-responsive T_H1 cells of patients with CD who are ASCA$^+$ have cytotoxic effector functions that result in potent killing ability of IECs in vitro. IECs have been reported to function as nonconventional antigen-presenting cells (APCs), presenting antigens for intestinal microorganisms[36]. It is therefore tempting to speculate that yeast-reactive T_H1-CTLs might promote killing of IECs in vivo and thus could be involved in intestinal barrier deterioration in patients with CD, which needs further investigation.

Yeast-reactive CD4$^+$ T cells are altered in IBD-FDRs

So far, it remains unclear whether the development of yeast-responsive T_H1-CTLs is a consequence of the disease or could eventually contribute to disease development and/or exacerbation. To address potential alterations of yeast-responsive T cells already in a predisease state, we analyzed a cohort of first-degree relatives of patients with IBD (IBD-FDRs), who have increased risk of developing IBD themselves[37,38]. We detected neither increased frequency nor increased IL-17A production of *C. tropicalis*- and *S. cerevisiae*-reactive T cells in IBD-FDRs compared with non-FDR controls (Extended Data Fig. 6a,b). However, *C. tropicalis*- and *S. cerevisiae*-reactive T cells from IBD-FDRs showed significantly increased IFN-γ production (Extended Data Fig. 6c,d), although less pronounced than for patients with CD (Fig. 2), whereas *Escherichia coli*-reactive cells, used as a control, were not altered (Extended Data Fig. 6c). In contrast to IFN-γ, cytotoxic markers were not significantly increased compared with non-FDR controls (Extended Data Fig. 6e). However, individual IBD-FDRs showed clearly elevated

levels of CD319 and PRF1 on *C. tropicalis*- and/or *S. cerevisiae*-reactive T cells, whereas GZMB and CCL4 remained unchanged (Extended Data Fig. 6f). ASCA antibodies have been reported as a predictive biomarker that can be detected several years before the clinical diagnosis of CD[39,40]. Within our limited number of IBD-FDRs, we identified individuals with increased serum levels of ASCA IgG and IgA (Extended Data Fig. 6g). As for patients with CD, increased expression of cytotoxic markers was associated with elevated ASCA antibody titers in IBD-FDRs (Extended Data Fig. 6h).

In summary, these data indicate that a skewing toward a T_H1 cell phenotype of yeast-responsive T cells is already detectable in IBD-FDRs and thus before the clinical onset of IBD. They further suggest that the additional acquisition of cytotoxic effector functions may evolve progressively, maybe as a result of a more intense or sustained interaction with yeast antigens, due to increased intestinal permeability, which has been described in IBD-FDRs[41].

Clonally expanded T_H1-CTLs cross-react to multiple yeast species

Our data so far suggest that chronic antigen stimulation may foster T_H1-CTL development in patients with CD who are $ASCA^+$. To better understand how chronic exposure to a large variety of commensal and dietary fungi may affect the clonal composition of yeast-reactive T cells, we integrated T cell receptor (TCR) sequencing data from our scRNA-seq dataset. Indeed, T_H1-CTLs from patients with CD showed a massive expansion of individual clonotypes (Fig. 5a), further evidenced by a higher Gini's coefficient, as a measure of the evenness of a population (Fig. 5b). Strikingly, many of the *S. cerevisiae*-stimulated TCRs of patients with CD were shared with *C. tropicalis*- and *C. albicans*-stimulated cells, whereas shared TCRs for the different fungi were less abundant in healthy donors (Fig. 5c,d). Indeed, most of the strongly expanded clonotypes were shared between the TCR repertoires reactive against two or all three fungi (Fig. 5d). TCR cross-reactivity was most pronounced within the T_H1-CTL cluster, where >70% of the *S. cerevisiae*-reactive TCR-β sequences of patients with CD were also found in the *C. tropicalis*- and *C. albicans*-stimulated cells (Fig. 5e). This suggests that persistent or alternating exposure to conserved antigens present in different yeast species may promote the selective expansion of cross-reactive clonotypes. In particular, these cross-reactive clonotypes, but not clonotypes with a single species specificity, showed high expression of cytotoxic marker genes, as well as *HLA-DR* and *HOPX*, encoding for recent activation and chronic markers, respectively (Fig. 5f).

To further confirm the T cell cross-reactivity for individual TCRs, we re-expressed the most expanded cross-reactive T_H1-CTL TCRs from the single-cell dataset in primary T cells using clustered regularly interspaced palindromic repeats (CRISPR)–Cas9[42,43] (Extended Data Fig. 7a,b). The expanded TCR-transgenic T cells were re-challenged with a panel of different yeasts in the presence of autologous antigen-presenting cells (APCs). As shown in Fig. 5g–i, we observed high cross-reactivity of the transgenic T cells to several yeast species and the reactivity of individual TCRs further reflected the cross-reactivity pattern initially observed by TCR-seq (Fig. 5i). High cross-reactivity to several yeast species was also confirmed for ex vivo sorted and expanded, *S. cerevisiae*-reactive, cytotoxic, $CD154^+CD319^+$ single-cell clones (Fig. 5j). Finally, to validate the selective enrichment of cross-reactive cells in patients who were $ASCA^+$, we expanded bulk *C. albicans*-, *C. tropicalis*- and *S. cerevisiae*-reactive $CD154^+$ T_{mem} cells from patients with CD. Yeast-reactive T cells derived from patients with CD who are $ASCA^+$, but not $ASCA^-$, highly cross-reacted to various yeast species (Extended Data Fig. 7c,d), consistent with the presence of these cells in patients who are $ASCA^+$. Cytotoxic $CD4^+$ T cells have so far been mainly described in the context of persistent viral infections[32]. However, none of the TCR-transgenic T cells reacted to common viral antigens and we also observed no differences between patients with CD who are cytomegalovirus (CMV) positive and those who are CMV negative in the frequencies of yeast-responsive T cells (Extended Data Fig. 7e–g).

Taken together, these data show that $CD4^+$ T_H1-CTLs that cross-recognize various yeast species are strongly expanded in patients with CD who are $ASCA^+$. The repetitive encounter with conserved antigens, present in different yeast species, may thus lead to the selective expansion of the cross-reactive clones, which progress to cytotoxic cells owing to chronic stimulation in patients with CD.

$CD4^+$ T_H1-CTLs respond to food-derived yeast antigens

The finding of a substantial cross-recognition of various yeast species by the $CD4^+$ T_H1-CTLs prompted us to investigate potential further antigenic triggers of these cells. As several yeast species are widespread organisms and frequently consumed with the diet, we hypothesized that food-derived yeast species could also promote the activation of $CD4^+$ T_H1-CTLs from patients with CD. Cheese contains live microorganisms, including various *Candida*, *Saccharomyces, Penicillium* and several other fungal species[44,45]. To analyze whether food-derived fungal species could activate $CD4^+$ T_H1-CTLs in patients with CD, we stimulated PBMCs with heat-inactivated lysates of common cheese types and analyzed the reactive T cells by ARTE. Patients with CD who are $ASCA^+$, but not healthy donors, showed clearly increased reactivity, especially to the mold-ripened cheeses camembert and gorgonzola (Fig. 6a,b). In line with our previous results, these cheese-activated T cells from patients with CD produced increased amounts of IFN-γ (Fig. 6b) and expressed elevated levels of cytotoxic markers (Fig. 6c). To confirm that the T cell reactivity observed with the cheese lysates was the result of T cell cross-reactivity against yeasts, we expanded gorgonzola-activated $CD154^+$ T_{mem} cells and restimulated them with different microbial species. Indeed, expanded T cell lines from patients with CD who are $ASCA^+$ exhibited up to 100% cross-reactivity to several yeast species, but not bacteria or milk proteins (Fig. 6d,e), indicating that the observed reactivity against the cheese is probably directed

Fig. 5 | Clonally expanded T_H1-CTLs are cross-reactive to multiple yeast species. a, TCR-β clonotype sizes were overlaid with UMAP visualization of the scRNA-seq dataset. **b**, Gini's coefficient according to the different T cell clusters, depicting the distribution of TCR-β sequences (0 is total equality, that is, all clones have the same proportion; 1 is total inequality, that is, a population dominated by a single clone). To account for the uneven distribution of total sorted cells by samples, a down-sampled dataset was used taking 500 cells at random from each individual per fungal antigen (HD, $n = 3$; CD, $n = 3$). **c**, Number of T cells found in response to two or all three yeasts in healthy donors and patients with CD. The colors correspond to the different gene expression clusters from **a**. **d**, Clonal networks of antifungal TCR repertoires. Each dot represents a clonotype as defined by the TCR-β sequence. Connecting lines show TCR-β sequences that are shared between antifungal repertoires. The size of dots indicates clonal expansion. **e**, Percentage of identical TCR-β sequences found in samples stimulated with the different yeast species. **f**, Expression of selected marker genes according to TCR specificity. Colors represent the normalized mean expression levels and size indicates the proportion of cells expressing the respective genes. **g**, Cross-reactive TCRs from the single-cell dataset inserted into primary T cells using orthotopic TCR replacement. Dot plot examples show restimulation of expanded TCR-transgenic T cells for one TCR-α/β construct; numbers indicate percentage of reactive $CD154^+TNF^+$. **h**, Restimulation of TCR-transgenic T cells ($n = 7$) with different fungal species. **i**, Heatmap depicting the cross-reactivity of the individual TCR-transgenic T cells ($n = 7$) in relation to stimulation with *S. cerevisiae*. The initial observed cross-reactivity based on TCR-seq is indicated on the right. **j**, *S. cerevisiae*-reactive, cytotoxic, $CD154^+CD319^+$, single-cell clones ($n = 10$) sorted ex vivo, expanded and restimulated with different fungal species. The percentage of cross-reactivity is indicated in relation to stimulation with *S. cerevisiae*. Each symbol in **b** represents one individual donor, in **h** one TCR-transgenic T cell line and in **j** one T cell clone. Truncated violin plots with quartiles and range are shown in **b** and **j**.

https://doi.org/10.1038/s41591-023-02556-5

against the yeast species present in it. This was further confirmed by reactivity of the TCR-transgenic cells against the gorgonzola lysate (Fig. 6f,g), as well as against the yeast *Kluyveromyces lactis* (formerly *Saccharomyces lactis*), whereas reactivity to phylogenetic distant *Penicillium* or *Geotrichum* mold species, which are also frequently contained in cheese[44,45], was low.

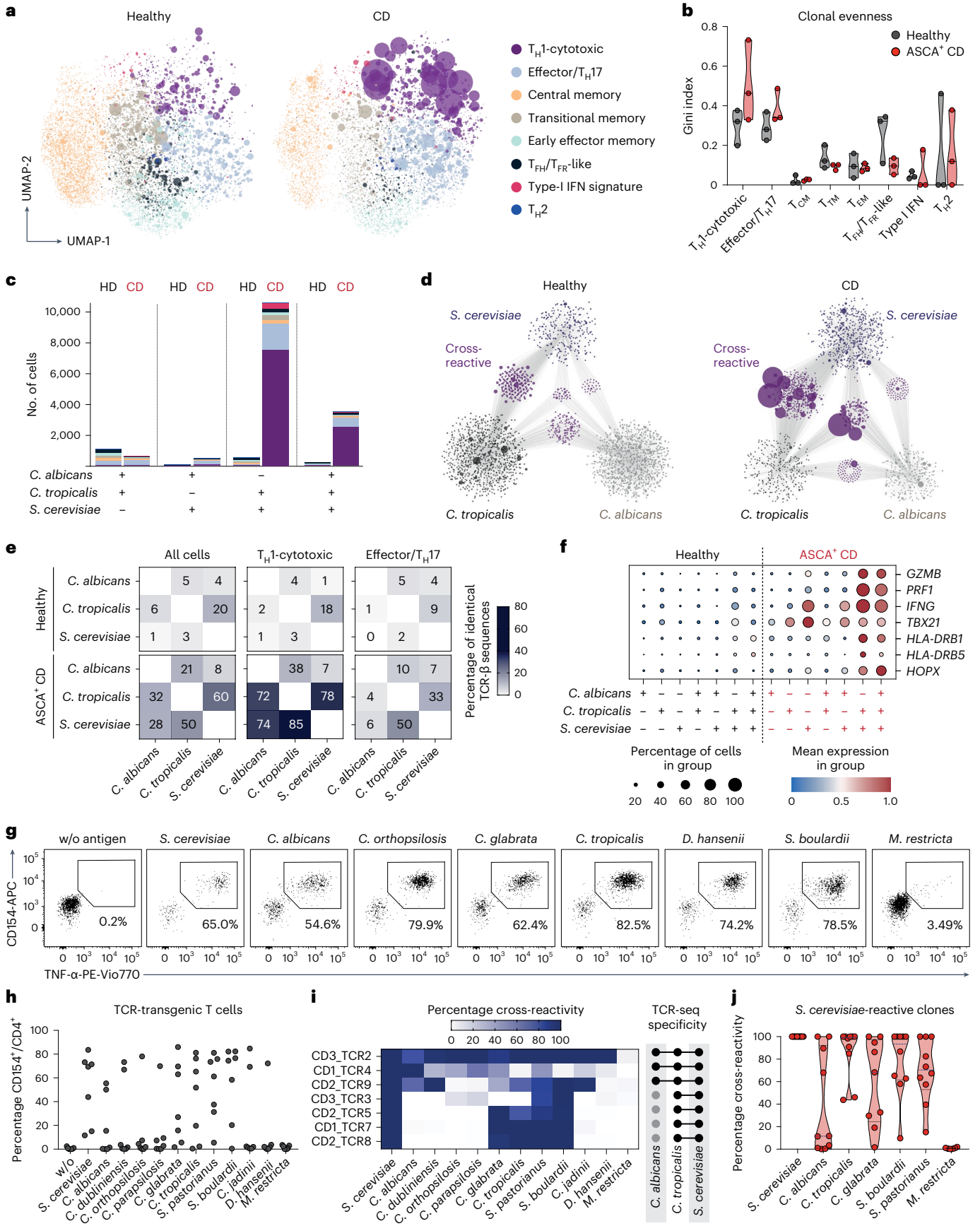

https://doi.org/10.1038/s41591-023-02556-5

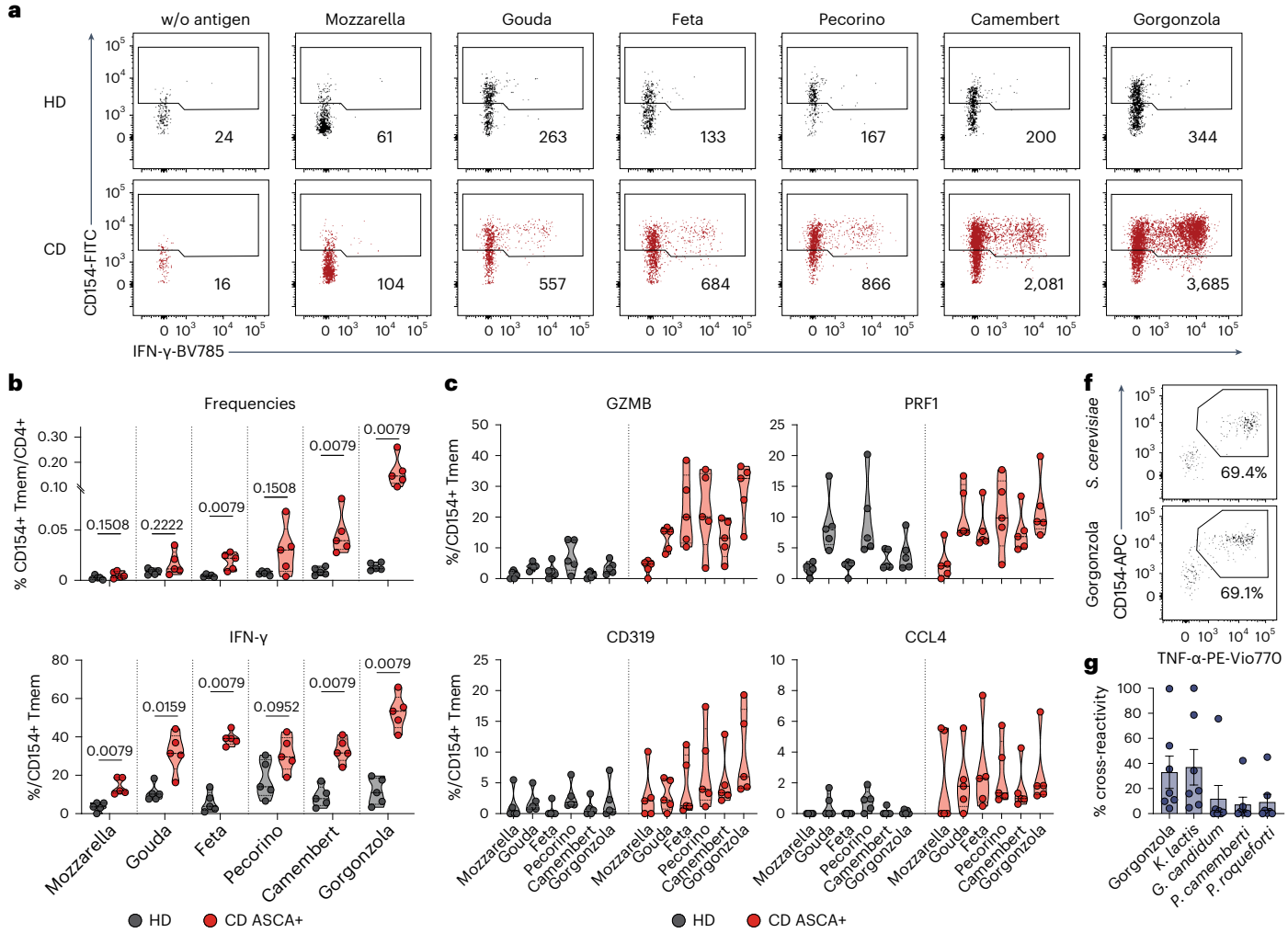

Fig. 6 | Food-derived yeasts can activate cross-reactive T_H1-CTLs in patients with CD. a–**c**, PBMCs of healthy donors and patients with CD were stimulated with lysates of different cheese types and reactive CD4$^+$ T cells analyzed by ARTE. **a**, Dot plot examples. Absolute cell counts after magnetic CD154$^+$ enrichment from 1×10^7 PBMCs are indicated. **b**, CD154$^+$ T_{mem} cell frequencies and IFN-γ production in response to different cheese types (HD, $n = 5$; ASCA$^+$ CD, $n = 5$). **c**, Ex vivo cytotoxic marker expression of reactive CD154$^+$ T_{mem} cells in response to different cheese types (HD, $n = 5$; ASCA+ CD, $n = 5$). **d**, Reactive CD154$^+$ T_{mem} cells from patients with CD who are ASCA$^+$ were isolated after stimulation with gorgonzola lysate and expanded. Dot plots show reactivity on restimulation with the indicated antigens. **e**, Cross-reactivity of expanded gorgonzola-activated cells from patients with CD who are ASCA$^+$ to different microbial and control antigens (*Kluyveromyces lactis*, *Penicllium camemberti*, *P. roqueforti*, *Geotrichum candidum*, $n = 2$; all other antigens, $n = 6$). **f**,**g**, TCR-transgenic T cells restimulated with lysates of gorgonzola or different fungal species commonly found in cheese. **f**, Dot plot examples with percentage of reactive CD154$^+$TNF$^+$ cells shown for one TCR-α/β construct. **g**, Cross-reactivity of the individual TCR-transgenic T cells ($n = 7$) in relation to stimulation with *S. cerevisiae*. Each symbol in **b**, **c** and **e** represents one individual donor and in **g** one TCR-transgenic T cell line. Truncated violin plots with quartiles and range are shown in **b**, **c** and **e** and mean values with s.e.m. in **g**. Statistical differences were obtained using the two-tailed Mann–Whitney *U*-test in **b**.

In summary, our data reveal that, in addition to gut-resident commensals, food-derived yeasts can also activate the cytotoxic T_H1-CTLs in patients with CD. The selective expansion of cross-reactive $CD4^+$ T cells by different members of the mycobiota, as identified in the present study, may contribute to chronicity and treatment resistance of CD, when persistently activated by different commensal and food-derived fungi.

Discussion

An inappropriate immune response against intestinal microorganisms has been suggested as a major contributor to the pathophysiology of CD. Despite extensive data supporting the involvement of T cells in IBD pathogenesis, the relevant intestinal antigens and the effector functions of the corresponding antigen-specific T cells, remain largely unknown. In the present study, we provide direct evidence that common intestinal fungal commensals, as well as food-derived yeasts, contribute to aberrant inflammatory $CD4^+$ T cell responses in patients with CD.

We observed massively increased $CD4^+$ T cell responses against different yeast species in patients with CD. In addition to *C. albicans*, which has been identified as a strong modulator of human adaptive immunity[15–17,22,46], the altered T cell response against non-*albicans Candida* and food-associated *Saccharomyces* spp. adds an additional layer to the inflammatory immune reaction in CD. Development of pathogenic T_H17 cells has been discussed as contributing to IBD pathology and we recently showed that *C. albicans* is the major driver of fungus-induced homeostatic T_H17 cell responses in humans[15]. In the present study, we observed that the proportion of T_H17 cells against *C. albicans* was surprisingly unaffected in patients with CD, but that cytotoxic T_H1 cells develop that also strongly react against non-*albicans Candida* spp., as well as different *Saccharomyces* yeasts. Which fungal species is the initial trigger of the T_H1 response and which fungi merely drive the selection of cross-reactive TCR remains unresolved. Recently, *Debaryomyces hansenii*, a yeast commonly contained in dairy products, has been described as being specifically enriched in inflamed wounds of patients with CD[18], suggesting that food-derived fungi may also adapt to the altered environment in the IBD gut. In this way, both intestinal fungal commensals and food-derived species could be involved in the initial priming of the T_H1 cell response observed here. Once established, these T_H1 cells may be propagated by multiple fungal species, leading to the evolution of a highly selected cross-reactive TCR repertoire.

The limited impact of IBD on the T_H17 cell reaction against *C. albicans* suggests that the strong homeostatic T_H17 cell response present in most individuals[15] is relatively inert to perturbations. Why T_H17 cell responses against *C. albicans* are less affected by IBD remains unclear. It is possible that fungus-reactive T_H1 and T_H17 cells recognize different antigens that have different availability in CD than in healthy individuals. Indeed, we detected high TCR cross-reactivity within the yeast-responsive T_H1-CTLs, compared with T_H17 cells. This indicates that T_H1-CTLs, but not T_H17 cells, are directed against conserved epitopes that are commonly present in many yeast species, thereby also increasing antigen abundance. Alternatively, a conversion of T_H17 into T_H1 cells may occur on continuous antigen stimulation in chronic inflammation[5,34]. However, yeast-reactive T_H17 and T_H1 cell cytokines were mainly produced by different cell populations and only small populations of IL-$17A^+$FN-γ^+ cells develop against non-*albicans Candida* and *Saccharomyces* spp. Altogether this suggests that T_H17 cells and T_H-CTLs represent two independent populations driven most probably by separated groups of antigens. In future studies, it will be important to define specific fungal proteins and peptides that are recognized by T_H17 cells and cross-reactive T_H-CTLs, which may allow the development of targeted, antigen-specific, therapeutic modulations. The cross-recognized antigens could comprise precisely the same or similar epitopes present in different yeast species or even unrelated sequences forming structurally similar epitopes, which moreover could also vary for different TCRs.

Overall, our data suggest a model in which, after initial T_H1 cell priming, repeated exposure to conserved antigens present in multiple fungal species leads to the selection of a highly cross-reactive TCR repertoire, accompanied by the acquisition of cytotoxic effector functions, probably as a result of chronic T cell activation. This is also supported by the observation that increased IFN-γ production and certain cytotoxic markers were elevated on yeast-responsive T cells in individual IBD-FDRs, but not yet the entire cytotoxic phenotype. Furthermore, the most expanded cross-reactive clonotypes from patients with CD showed the highest gene expression of cytotoxic markers, as well as the chronic activation marker gene *HOPX*[33,34]. As healthy individuals also harbor commensal intestinal yeasts and frequently ingest *S. cerevisiae* in the diet, the observed altered T cell reactivity in patients with CD and the incipient changes in individual IBD-FDRs may reflect a more intense or sustained interaction with yeast antigens, owing to epithelial barrier dysfunction. T cell-mediated cytotoxicity has been described as contributing to IEC death[47,48] and exacerbated T_H1 immunity in mice promoted epithelial barrier defects and mucosal fungal infection[49]. It is therefore tempting to speculate that yeast-responsive T_H-CTLs may be directly involved in disease initiation and/or exacerbation through disruption of the intestinal barrier. In this regard, cross-reactive, yeast-responsive TCRs could be prime targets for the development of specific therapeutic interventions by antigen-specific regulatory T cell (T_{reg} cell) therapy or T cell-depleting strategies.

Yeast-reactive T cells were selectively altered in patients with CD who are $ASCA^+$, but not in those who are $ASCA^-$ or in patients with UC. It is thus possible that yeast-reactive T_H-CTLs or their T_H1 progenitors may be involved in providing B cell help for ASCA formation. The presence of ASCAs in CD was described more than 30 years ago[50,51] and ASCAs are used as a biomarker for disease severity[30], as well as a prognostic marker in individuals at risk for developing IBD[40]. Despite this strong link, their direct pathogenic relevance has been questioned and the yeast-responsive T cells have so far not been analyzed in detail in patients with CD. *S. cerevisiae*, also known as bakers' yeast, is ingested daily via nutritional intake and therefore generally considered to have a low virulence in humans. Instead, *C. albicans*, due to its higher immunogenicity, has been speculated to be the inducing species, as a result of binding of ASCAs to *C. albicans* mannans[24]. Given the data presented in the present study, it will be important to further define the fungal species and mechanisms involved in ASCA formation and in particular the contribution of T_H1-CTLs.

Our data may also result in concepts for selecting patients with CD for particular therapies. For example, therapeutic inhibition of Janus kinases targets, among other cytokines, the release of IFN-γ and might show more effectivity in patients with CD who are $ASCA^+$. Further studies will examine the role of nutritional interventions with selective removal of yeast antigens, which—if effective—would be an attractive treatment strategy supporting the efficacy of other anti-inflammatory therapies or remission maintenance. Antifungal therapy, as well as a yeast-free diet, will be analyzed in future clinical trials in patients with CD who are $ASCA^+$.

Our study also has some limitations. Although we have provided strong correlative evidence for the involvement of yeast-reactive $CD4^+$ T cells in CD, further investigations are necessary to determine their direct contribution to disease pathophysiology. Our initial attempts in this direction provide some encouraging results and evidence for the ability of these cells to directly kill intestinal epithelium in vitro. However, further studies need to clarify whether therapeutic targeting of intestinal yeasts or yeast-responsive T_H1-CTLs is clinically effective. Although these highly cross-reactive T cells in patients with CD react to multiple yeast species, future studies are needed to determine whether a single or multiple species serve as the initial trigger for the altered

yeast-reactive T cell response. In the present study, we analyzed only a limited number of bacterial and fungal species and potential differences induced by strain variation were not addressed. Furthermore, the proteins or peptides driving the cross-reactive, yeast-responsive population remain to be determined. The discovery that a specific subgroup of patients with CD develops altered $CD4^+$ T cell responses and ASCAs against yeasts, whereas other patients with IBD do not, underscores the presence of fundamentally distinct host–microbe interactions within this subgroup of patients. This emphasizes the need for in-depth investigations to shed light on the underlying mechanisms and to discern the unique characteristics of this subgroup of patients with CD.

Online content

Any methods, additional references, Nature Portfolio reporting summaries, source data, extended data, supplementary information, acknowledgements, peer review information; details of author contributions and competing interests; and statements of data and code availability are available at https://doi.org/10.1038/s41591-023-02556-5.

References

1. Schmitt, H., Neurath, M. F. & Atreya, R. Role of the IL23/IL17 pathway in Crohn's disease. *Front. Immunol.* **12**, 622934 (2021).
2. Sewell, G. W. & Kaser, A. Interleukin-23 in the pathogenesis of inflammatory bowel disease and implications for therapeutic intervention. *J. Crohns Colitis* **16**, ii3–ii19 (2022).
3. Hueber, W. et al. Secukinumab, a human anti-IL-17A monoclonal antibody, for moderate to severe Crohn's disease: unexpected results of a randomised, double-blind placebo-controlled trial. *Gut* **61**, 1693–1700 (2012).
4. Targan, S. R. et al. A randomized, double-blind, placebo-controlled phase 2 study of brodalumab in patients with moderate-to-severe Crohn's disease. *Am. J. Gastroenterol.* **111**, 1599–1607 (2016).
5. Schnell, A., Littman, D. R. & Kuchroo, V. K. T_H17 cell heterogeneity and its role in tissue inflammation. *Nat. Immunol.* **24**, 19–29 (2023).
6. Tindemans, I., Joosse, M. E. & Samsom, J. N. Dissecting the heterogeneity in T-cell mediated inflammation in IBD. *Cells* **9**, 110 (2020).
7. Alexander, K. L. et al. Human microbiota flagellins drive adaptive immune responses in Crohn's disease. *Gastroenterology* **161**, 522–535.e526 (2021).
8. Calderon-Gomez, E. et al. Commensal-specific $CD4^+$ cells from patients with Crohn's disease have a T-helper 17 inflammatory profile. *Gastroenterology* **151**, 489–500.e3 (2016).
9. Ergin, A. et al. Impaired peripheral Th1 CD4+ T cell response to *Escherichia coli* proteins in patients with Crohn's disease and ankylosing spondylitis. *J. Clin. Immunol.* **31**, 998–1009 (2011).
10. Hegazy, A. N. et al. Circulating and tissue-resident $CD4^+$ T cells with reactivity to intestinal microbiota are abundant in healthy individuals and function is altered during fnflammation. *Gastroenterology* **153**, 1320–1337.e1316 (2017).
11. Morgan, N. N. et al. Crohn's Disease patients uniquely contain inflammatory responses to flagellin in a CD4 effector memory subset. *Inflamm. Bowel Dis.* **28**, 1893–1903 (2022).
12. Morgan, N. N. & Mannon, P. J. Flagellin-specific CD4 cytokine production in Crohn disease and controls is limited to a small subset of antigen-induced $CD40L^+$ T cells. *J. Immunol.* **206**, 345–354 (2021).
13. Pedersen, T. K. et al. The $CD4^+$ T cell response to a commensal-derived epitope transitions from a tolerant to an inflammatory state in Crohn's disease. *Immunity* **55**, 1909–1923.e6 (2022).
14. Shen, C., Landers, C. J., Derkowski, C., Elson, C. O. & Targan, S. R. Enhanced CBir1-specific innate and adaptive immune responses in Crohn's disease. *Inflamm. Bowel Dis.* **14**, 1641–1651 (2008).
15. Bacher, P. et al. Human anti-fungal Th17 immunity and pathology rely on cross-reactivity against *Candida albicans*. *Cell* **176**, 1340–1355.e1315 (2019).
16. Doron, I. et al. Human gut mycobiota tune immunity via CARD9-dependent induction of anti-fungal IgG antibodies. *Cell* **184**, 1017–1031.e1014 (2021).
17. Doron, I. et al. Mycobiota-induced IgA antibodies regulate fungal commensalism in the gut and are dysregulated in Crohn's disease. *Nat. Microbiol.* **6**, 1493–1504 (2021).
18. Jain, U. et al. Debaryomyces is enriched in Crohn's disease intestinal tissue and impairs healing in mice. *Science* **371**, 1154–1159 (2021).
19. Leonardi, I. et al. Mucosal fungi promote gut barrier function and social behavior via type 17 immunity. *Cell* **185**, 831–846 e814 (2022).
20. Li, X. V. et al. Immune regulation by fungal strain diversity in inflammatory bowel disease. *Nature* **603**, 672–678 (2022).
21. Limon, J. J. et al. Malassezia is associated with Crohn's disease and exacerbates colitis in mouse models. *Cell Host Microbe* **25**, 377–388.e376 (2019).
22. Ost, K. S. et al. Adaptive immunity induces mutualism between commensal eukaryotes. *Nature* **596**, 114–118 (2021).
23. Acosta-Rodriguez, E. V. et al. Surface phenotype and antigenic specificity of human interleukin 17-producing T helper memory cells. *Nat. Immunol.* **8**, 639–646 (2007).
24. Gerard, R., Sendid, B., Colombel, J. F., Poulain, D. & Jouault, T. An immunological link between *Candida albicans* colonization and Crohn's disease. *Crit. Rev. Microbiol.* **41**, 135–139 (2015).
25. Auchtung, T. A. et al. Investigating colonization of the healthy adult gastrointestinal tract by fungi. *mSphere* **3**, e00092–18 (2018).
26. Nash, A. K. et al. The gut mycobiome of the human microbiome project healthy cohort. *Microbiome* **5**, 153 (2017).
27. Raimondi, S. et al. Longitudinal survey of fungi in the human gut: Its profiling, phenotyping, and colonization. *Front. Microbiol.* **10**, 1575 (2019).
28. Bacher, P. et al. Antigen-reactive T cell enrichment for direct, high-resolution analysis of the human naive and memory Th cell repertoire. *J. Immunol.* **190**, 3967–3976 (2013).
29. Sokol, H. et al. Fungal microbiota dysbiosis in IBD. *Gut* **66**, 1039–1048 (2017).
30. Ferrante, M. et al. New serological markers in inflammatory bowel disease are associated with complicated disease behaviour. *Gut* **56**, 1394–1403 (2007).
31. Sivananthan, K. & Petersen, A. M. Review of *Saccharomyces boulardii* as a treatment option in IBD. *Immunopharmacol. Immunotoxicol.* **40**, 465–475 (2018).
32. Preglej, T. & Ellmeier, W. $CD4^+$ cytotoxic T cells—phenotype, function and transcriptional networks controlling their differentiation pathways. *Immunol. Lett.* **247**, 27–42 (2022).
33. Albrecht, I. et al. Persistence of effector memory Th1 cells is regulated by Hopx. *Eur. J. Immunol.* **40**, 2993–3006 (2010).
34. Maschmeyer, P. et al. Immunological memory in rheumatic inflammation—a roadblock to tolerance induction. *Nat. Rev. Rheumatol.* **17**, 291–305 (2021).
35. Trapnell, C. et al. The dynamics and regulators of cell fate decisions are revealed by pseudotemporal ordering of single cells. *Nat. Biotechnol.* **32**, 381–386 (2014).
36. Heuberger, C. E. et al. MHC class II antigen presentation by intestinal epithelial cells fine-tunes bacteria-reactive CD4 T cell responses. *Mucosal Immunol.* (in the press).
37. Halfvarson, J. et al. Age determines the risk of familial inflammatory bowel disease—a nationwide study. *Aliment. Pharm. Ther.* **56**, 491–500 (2022).
38. Halme, L. et al. Family and twin studies in inflammatory bowel disease. *World J. Gastroenterol.* **12**, 3668–3672 (2006).

39. Choung, R. S. et al. Preclinical serological signatures are associated with complicated Crohn's disease phenotype at diagnosis. *Clin. Gastroenterol. Hepatol.* https://doi.org/10.1016/j.cgh.2023.01.033 (2023).
40. Torres, J. et al. Serum biomarkers identify patients who will develop inflammatory bowel diseases up to 5 years before diagnosis. *Gastroenterology* **159**, 96–104 (2020).
41. Keita, A. V. et al. Gut barrier dysfunction—a primary defect in twins with Crohn's disease predominantly caused by genetic predisposition. *J. Crohns Colitis* **12**, 1200–1209 (2018).
42. Moosmann, C., Muller, T. R., Busch, D. H. & Schober, K. Orthotopic T-cell receptor replacement in primary human T cells using CRISPR–Cas9-mediated homology-directed repair. *STAR Protoc.* **3**, 101031 (2022).
43. Schober, K. et al. Orthotopic replacement of T-cell receptor alpha- and beta-chains with preservation of near-physiological T-cell function. *Nat. Biomed. Eng.* **3**, 974–984 (2019).
44. Büchl, N. R. & Seiler, H. Yeasts and molds: Yeasts in milk and dairy products. In *Encyclopedia of Dairy Sciences*, 2nd edn (eds Fuquay, J. W., Fox, P.F. & McSweeney, P. L. H.) pp 744–753 (2011).
45. Wolfe, B. E., Button, J. E., Santarelli, M. & Dutton, R. J. Cheese rind communities provide tractable systems for in situ and in vitro studies of microbial diversity. *Cell* **158**, 422–433 (2014).
46. Zielinski, C. E. et al. Pathogen-induced human TH17 cells produce IFN-gamma or IL-10 and are regulated by IL-1beta. *Nature* **484**, 514–518 (2012).
47. Brabec, T. et al. Epithelial antigen presentation controls commensal-specific intraepithelial T-cells in the gut. Preprint at *bioRxiv* https://doi.org/10.1101/2022.08.21.504672 (2022).
48. Merger, M. et al. Defining the roles of perforin, Fas/FasL, and tumour necrosis factor alpha in T cell induced mucosal damage in the mouse intestine. *Gut* **51**, 155–163 (2002).
49. Break, T. J. et al. Aberrant type 1 immunity drives susceptibility to mucosal fungal infections. *Science* **371**, eaay5731 (2021).
50. Main, J. et al. Antibody to Saccharomyces cerevisiae (bakers' yeast) in Crohn's disease. *Br. Med. J.* **297**, 1105–1106 (1988).
51. McKenzie, H., Main, J., Pennington, C. R. & Parratt, D. Antibody to selected strains of Saccharomyces cerevisiae (baker's and brewer's yeast) and *Candida albicans* in Crohn's disease. *Gut* **31**, 536–538 (1990).

[1]Institute of Immunology, Christian-Albrechts-University of Kiel and University Medical Center Schleswig-Holstein, Kiel, Germany. [2]Institute of Clinical Molecular Biology, Christian-Albrechts-University of Kiel and University Medical Center Schleswig-Holstein, Kiel, Germany. [3]The Jill Roberts Institute for Research in Inflammatory Bowel Disease, Weill Cornell Medicine, Cornell University, New York, NY, USA. [4]Joan and Sanford I. Weill Department of Medicine, Weill Cornell Medicine, Cornell University, New York, NY, USA. [5]Department of Microbiology and Immunology, Weill Cornell Medicine, Cornell University, New York, NY, USA. [6]Department of Internal Medicine I, University Medical Center Schleswig-Holstein, Kiel, Germany. [7]Institute of Epidemiology, Christian-Albrechts-University of Kiel and popgen Biobank, University Medical Center Schleswig-Holstein, Kiel, Germany. [8]Gastroenterologie am Bayerischen Platz, Berlin, Germany. [9]Department of Gastroenterology, Rheumatology and Infectious Diseases, Charité-Universitätsmedizin Berlin, Humboldt-Universität zu Berlin and Berlin Institute of Health, Berlin, Germany. [10]Gastroenterology–Hepatology Center Kiel, Kiel, Germany. [11]Institute of Microbiology, Infectious Diseases and Immunology, Charité-Universitätsmedizin Berlin, Humboldt-Universität zu Berlin and Berlin Institute of Health, Berlin, Germany. [12]Department of Infectious Diseases and Microbiology, University of Lübeck, Lübeck, Germany. [13]Department of Molecular and Applied Microbiology, Leibniz Institute for Natural Product Research and Infection Biology—Hans Knoell Institute, Jena, Germany. [14]Friedrich Schiller Universität, Jena, Germany. [15]Institute of Microbiology, Department of Microbial Pathogenicity Mechanisms, Leibniz Institute for Natural Product Research and Infection Biology—Hans Knoell Institute, Jena, Germany. ✉e-mail: p.bacher@ikmb.uni-kiel.de

Methods

Blood donors

Peripheral EDTA blood samples of healthy donors were obtained from blood bank donors of the Institute for Transfusion Medicine, UKSH Kiel, Germany or from in-house volunteers (ethics committee CAU Kiel D578/18, D427/19). Peripheral EDTA blood samples from patients with IBDs were obtained from the Department of Internal Medicine I, UKSH Kiel, the Comprehensive Center for Inflammation Medicine and the Gastroenterology–Hepatology Center Kiel (ethics committee CAU Kiel D427/19). IBD-FDRs were recruited from the Kiel IBD Family Cohort Study, a German-wide cohort of patients with IBD and their family members (ethics committee CAU Kiel A117/13), built by the popgen Biobank at Kiel University/University Hospital SH in Kiel. Demographic data about the study participants are provided in Extended Data Tables 1 and 2. CMV serostatus was determined using an anti-CMV IgG ELISA according to the manufacturer's instructions (Serion Diagnostics). All blood donors gave written informed consent before participation.

Intestinal biopsies

Biopsies from inflamed and noninflamed intestinal tissue were collected from patients with CD who underwent colonoscopy (ethics committee CAU Kiel, under the file: B 231/89-1/13). All patients gave written informed consent before participation.

Small IECs

Primary small IECs were purchased from PELOBiotech. Cells were cultivated in Epithelial Cell Medium (Cell Biologics) in T25 flasks pretreated with gelatin-based coating solution (Cell Biologics). During expansion, medium was replenished and cells were split as needed.

Quantification of ASCAs

Serum ASCAs were measured by ELISA according to the manufacturer's instructions (Euroimmun). In short, ASCA IgA/IgG ELISA kits include three calibration sera, a positive and a negative control. Sera were diluted 1:101 in probe buffer and incubated at room temperature on precoated microtiter plates for 30 min. After washing, a peroxidase-conjugated, anti-human IgA or IgG was added for 30 min and the plates were washed again. Substrate solution was added and the color reaction was stopped after 15 min. The optical density was determined at 450 nm, with a reference wavelength of 620 nm. ASCA status was calculated after developing a standard curve using the three calibration sera. ASCA quantification was done in duplicate and mean values were used. Sera were considered positive if their activity was >20 relative units ml^{-1}. Both single-positive IgA or IgG samples and double-positive samples were classified as $ASCA^{+}$ donors.

ITS-sequencing

ITS (internal transcribed spacer) amplicons were generated with 35 cycles using Invitrogen AccuPrime PCR reagents. These amplicons were used in a second PCR reaction, applying Illumina Nextera XT v.2 (Illumina) barcoded primers to uniquely index each sample as previously described[20]. All libraries were processed for quality control using the DNA 1000 Bioanalyzer (Agilent) and Qubit (Life Technologies) to validate and quantify library construction before preparing a paired-end flow cell. The samples were randomly divided among flow cells to minimize sequencing bias. Clonal bridge amplification (Illumina) was performed using a cBot (Illumina); 2× 250-base pair (bp) sequencing-by-synthesis was performed using the Illumina MiSeq platform.

Generation of microbial antigen lysates

Bacterial and fungal lysates were generated according to previously described methods[15,52]. In brief, bacteria *E. coli* (DSM 8698), *Faecalibacterium prausnitzii* (DSM 17677), *Bacteroides fragilis* (American Type Culture Collection (ATCC) 25285), *Clostridium leptum* (DSM 753), *Prevotella copri* (DSM 18205), *Akkermansia muciniphila* (DSM 22959) and *Klebsiella pneumoniae* (clinical isolate) were grown on solid medium (Columbia Blood Agar, Biomérieux), harvested by scraping into 17.4 ml of distilled water and lysed by addition of 0.4 ml of NaOH (1 M), 0.2 ml of HCl (2 M) and 2 ml of 10× phosphate-buffered saline (PBS), pH 7.5. Lysis of cells was confirmed by microscopic analysis and by negative culture of lysates. Heat-killed *Lactobacillus rhamnosus* was purchased from Invivogen.

Lyophilized extract of *C. albicans* (SN-16946) was purchased from Greer Laboratories. *S. cerevisiae* (ATCC 9763), *S. boulardii* (Perenterol), *S. pastorianus* (DSM 6580), *Cyberlindnera jadinii* (CBS 1600), *C. dubliniensis* (CD36), *C. tropicalis* (DSM 11953), *Candida glabrata* (ATCC 2001), *C. parapsilosis* (GA1), *C. orthopsilosis* (ATCC 96141), *Debaryomyces hansenii* (JMRC STI25082), *K. lactis* (formerly *S. lactis*; STH00086) and *G. candidum* (SF012383) were first grown on yeast–peptone–dextrose (YPD) agar plates (10 g l^{-1} of peptone, 5 g l^{-1} of yeast extract, 20 g l^{-1} of dextrose and 15 g l^{-1} of agar). For protein extraction, liquid cultures of *S. pastorianus* and *C. jadinii* were grown in synthetic defined (SD) medium (2% glucose, 6.7 g l^{-1} of yeast nitrogen base without amino acids, 20 mg l^{-1} of histidine,120 mg l^{-1} of leucine, 60 mg l^{-1} of lysine, 20 mg l^{-1} of arginine, 20 mg l^{-1} of tryptophan, 20 mg l^{-1} of tyrosine, 40 mg l^{-1} of threonine, 20 mg l^{-1} of methionine, 50 mg l^{-1} of phenylalanine, 20 mg l^{-1} of uracil and 20 mg l^{-1} of adenine), *K. lactis* and *G. candidum* in SD + CSM (2% glucose, 6.7 g l^{-1} of yeast nitrogen base without amino acids, 1× complete supplement mixtures (CSM, Formedium)), *D. hansenii* in liquid Sabouraud 2% (w/v) glucose-bouillon (Carl Roth), and *C. dubliniensis*, *C. tropicalis*, *C. glabrata*, *C. parapsilosis* and *C. orthopsilosis* in liquid YPD medium overnight at 30 °C. *M. restricta* (CBS-7877) and *M. furfur* (DSM 6170) were cultured in 250 ml of MLNA medium (10 g l^{-1} of bacteriological peptone, 10 g l^{-1} of glucose, 2 g l^{-1} of yeast extract, 8 g l^{-1} of desiccated ox bile, 10 ml l^{-1} of glycerol, 0.5 g l^{-1} of glycerol monostearate, 5 ml l^{-1} of Tween-80 and 20 ml l^{-1} of olive oil) at 32 °C for 4 d.

Yeast cells were harvested by centrifugation for 5 min at ≥1,500*g* and washed 3× to remove culture medium. Cell pellets were disrupted in a tissue homogenizer with glass beads for at least three rounds at high intensity, with 5 min of incubation on ice in between. All microbial extracts were centrifuged at 15,000–20,000*g* for 1–15 min to remove debris, supernatants were passed through a 0.2-µm sterile filter (Sartorius, Minisart) and stored in aliquots at −70 °C until use.

Penicillium roqueforti (SF006507) and *P. camemberti* (STN02007) were cultivated at 20 °C for 7–10 d on malt agar plates and germinated in *Aspergillus* minimal medium with glucose as the sole carbon source at 24 °C until sufficient mycelial pellets were present. Mycelia were separated from the medium with Miracloth (Merck Millipore), washed with water and protein extracts were generated by breaking the mycelium in liquid nitrogen by grinding using a mortar and pestle.

To generate suspensions from cheese, cheeses were cut into small pieces and put into gentleMACS M-tubes (Miltenyi Biotec) containing 3 ml of 1× PBS buffer. Cheeses were disrupted using the gentleMACS device (Miltenyi Biotec) program RNA.01 3×. Tubes were centrifuged at 1,000*g* for 10 min and supernatants were heat inactivated for 10 min at 65 °C.

All microbial lysates were used in at a protein concentration of 40 µg ml^{-1} for stimulation and cheese suspensions were used at a protein concentration of 200 µg ml^{-1}.

Other antigens

The following control antigens were used for stimulation: lysates of CMV (Siemens Healthcare Diagnostics), adenovirus (AdV; Microbix), varicella-zoster virus (Microbix) and Epstein–Barr virus (Hölzel Biotech). All viral lysates were used at a concentration of 10 µg ml^{-1} for stimulation. Peptide pools of herpes simplex virus 1 (Envelope Glycoprotein D; Miltenyi Biotec), influenza A H1N1 (pool of HA, MP1, MP2, NP, NA; Miltenyi Biotec), human herpesvirus 6 (pool of U54, U90; peptides&elephants) and SARS-CoV-2 (spike protein; JPT). Peptide

pools were resuspended according to manufacturers' instructions and cells were stimulated at a concentration of 0.5 µg per peptide per ml. Cows' milk protein extract was purchased from Greer Laboratories and used at a concentration of 100 µg ml^{-1}.

Antigen-reactive T cell enrichment

PBMCs were freshly isolated from EDTA blood on the day of blood donation by density gradient centrifugation (Biocoll, Biochrom). ARTE was performed as previously described[15,28,52–54], with slight modifications. In brief, 1–2 × 10^7 PBMCs were plated in RPMI-1640 medium (Gibco), supplemented with 5% (v/v) human AB-serum (Sigma-Aldrich) in 12-well cell-culture plates and stimulated for 7 h with microbial lysates in the presence of 1 µg ml^{-1} of CD40 and 1 µg ml^{-1} of CD28 pure antibody (both Miltenyi Biotec). Then, 1 µg ml^{-1} of Brefeldin A (Sigma-Aldrich) was added for the last 2 h. In some experiments 100 µg ml^{-1} of anti-HLA-DR pure antibody (Miltenyi Biotec; clone AC122 or BioXcell; clone LT43) was added during stimulation. To multiplex several specificities, the differentially stimulated cells were labeled with different concentrations of two CD4 antibody clones (CD4-BV421, BioLegend, clone OKT4, titer 1:20 and 1:200; CD4-APC-Vio770, Miltenyi Biotec, clone MT-466, titers 1:50 and 1:500). For lower concentrations, the respective unconjugated CD4 pure antibody was added at a concentration of 1 µg ml^{-1} to block intermixing of the barcode label. Barcoded populations were pooled and labeled with CD154-biotin followed by anti-biotin MicroBeads (CD154 MicroBead Kit, Miltenyi Biotec) and magnetically enriched by two sequential MS Columns (Miltenyi Biotec). Surface staining was performed on the first column, followed by fixation and intracellular staining on the second column. Frequencies of antigen-specific T cells were determined based on the cell count of CD154$^+$ T cells after enrichment, normalized to the total number of CD4$^+$ T cells applied on the column. For each stimulation, CD154$^+$ background cells enriched from the nonstimulated control were subtracted.

Flow cytometry

Cells were stained in different combinations of fluorochrome-conjugated antibodies (clone names and titers in parentheses): CD3-PE (REA613), CD4-APC-Vio770 (M-T466), CD4-VioBlue (REA623), CD4-FITC (REA623), CD8-VioGreen (REA734), CD8-PerCP (BW135/80), CD14-VioGreen (REA599), CD14-PerCP (TÜK4), CD20-VioGreen (LT20), CD20-PerCP (LT20), CD45RA-VioGreen (REA562), CD45RO-APC (REA611), CD69-PE (REA824), CD154-FITC (REA238), CD154-APC (REA238), TNF (tumor necrosis factor)-PE (phycoerythrin)-Vio770 (cA2), CD197 (CCR7)-PE-Bio770 (REA108), IL-17A-PE-Vio770 (REA1063), IL-21-VioR667 (REA1039), IL-21-PE (REA1039), perforin-PE (REA1061), GM-CSF-APC (REA1215), GM-CSF-PE-Vio770 (REA1215) (all Miltenyi Biotec, all in titer 1:50), CD4-BV421 (OKT4, 1:20), CD45RA-PE-Cy5 (HI100, 1:60), IFN-γ-BV785 (4 S.B3, 1:20), IL-2-BV605 (MQ1-17H12, 1:20), IL-2-BV711 (MQ1-17H12, 1:50), IL-10-PE-Dazzle-594 (JES3-9D7, 1:50), IL-17A-BV605 (BL168, 1:20), Granzyme-B-PerCP-Cy5 (QA16A02, 1:20), CD319-PE-Dazzle-594 (162.1, 1:20), TNF-BV650 (MAb11, 1:20), anti-mouse-TCR-β-APC (H57-597, 1:20), anti-human-TCR-αβ-FITC (IP26, 1:20) (all BioLegend), and IL-17A-BV650 (N49-653, 1:20), integrin b7-BV650 (FIB504, 1:20), CCL4 (MIP-1b)-AF770-(D21-1351, 1:20), Ki-67-AF700 (B56, 1:20), Ki-67-BV480 (B56, 1:20) and IL-22-PerCP-eFluor710 (IL22JOP, 1:100) (all BD Biosciences). Viability 405/520 Fixable Dye 1:100 (Miltenyi Biotec) was used to exclude dead cells. For intracellular staining, cells were fixed and permeabilized with the inside stain kit (Miltenyi Biotec). Data were acquired on an LSR Fortessa (BD Bioscience) or Northern Lights 3000 (Cytek Biosciences). Screening of expanded T cell lines on 384-well plates was performed on a MACSQuantX Analyzer (Miltenyi Biotec). FlowJo v.10.9.0 (Tree Star) software was used for analysis.

Expansion and restimulation of antigen-reactive T cells

For expansion of antigen-specific T cells, PBMCs were stimulated for 6 h in the presence of 1 µg ml^{-1} of CD40 and 1 µg ml^{-1} of CD28 pure antibody, CD154$^+$ cells were isolated by magnetic activated cell sorting (MACS) and further purified by FACS on a FACS Aria Fusion (BD Bioscience) based on CD154$^+$CD69$^+$CD45RA$^-$ expression into 96-well, round-bottomed plates. For generation of yeast-responsive T_H1-CTL single-cell clones, *S. cerevisiae*-stimulated CD154$^+$CD69$^+$CD45RA$^-$CD319$^+$ cells were sorted by FACS as single cells into 96-well, round-bottomed plates.

Bulk or single-cell sorted T cells were expanded in the presence of 1 × 10^5 autologous, antigen-loaded irradiated feeder cells (negative fraction from CD154$^+$ MACS) in TexMACS medium (Miltenyi Biotec), supplemented with 5% (v/v) human AB-serum (GemCell), 200 U ml^{-1} of IL-2 (Proleukin; Novartis), 100 IU ml^{-1} of penicillin, 100 µg ml^{-1} of streptomycin, 0.25 µg ml^{-1} of amphotericin B (antibiotic antimycotic solution, Sigma-Aldrich), 20 µM 2-mercaptoethanol (Gibco, Life Technologies), 2 mM glutamine and 30 ng ml^{-1} of anti-CD3 (OKT-3; Miltenyi Biotec). After 7 d, 100 ml of the medium was replenished and 1 × 10^5 irradiated feeder cells were added. During expansion for 2–4 weeks, medium was replenished and cells were split as needed.

For restimulation, fastDCs were generated from autologous CD14$^+$ MACS-isolated monocytes (CD14 MicroBeads; Miltenyi Biotec) by cultivation in X-Vivo15 medium (BioWhittaker/Lonza), supplemented with 1,000 IU ml^{-1} of GM-CSF and 400 IU ml^{-1} of IL-4 (both Miltenyi Biotec). Before restimulation, expanded T cells were rested in RPMI-1640 supplemented with 5% human AB-serum without IL-2 for 2 d. Then, 0.5–1 × 10^5 expanded T cells were plated with fastDCs in a ratio of 1:1 of in 384-well, flat-bottomed plates and restimulated for 6 h, with 1 mg ml^{-1} of Brefeldin A added for the last 4 h. Cells were stained intracellularly for CD154 and cytokines.

Expansion of CD4$^+$ T cells from intestinal biopsies

Up to 4 biopsies per patient were pooled and digested in 1 mL of Hanks' balanced salt solution $Ca^{2+}Mg^{2+}$ (Gibco) supplemented with 0.5% (v/v) human AB-serum, 100 IU ml^{-1} of penicillin, 100 µg ml^{-1} of streptomycin, 0.25 µg ml^{-1} of amphotericin B, 10 IU ml^{-1} of DNase I (CellSystems) and 1 mg ml^{-1} of collagenase type CLS IV (Biochrom) for 30 min at 37 °C while shaking. Cells were filtered through a 40-µm cell strainer to remove aggregates and stained with fluorochrome-conjugated antibodies to CD4-VioBlue, CD3-PE, CD8-PerCP, CD14-PerCP, CD20-PerCP, CD45RO-APC and CCR7-PE-Vio770 (all Miltenyi Biotec). Each 200 CD3$^+$CD4$^+$CD45RO$^+$ cells were sorted in multiple wells of a 96-well plate containing irradiated allogeneic feeder cells in TexMACS medium, supplemented with 5% (v/v) human AB-serum, 200 U ml^{-1} of IL-2 and 100 IU ml^{-1} of penicillin, 100 µg ml^{-1} of streptomycin, 0.25 µg ml^{-1} of amphotericin B at a density of 2 × 10^5 cells cm^{-2}. Cells were polyclonally expanded for 4 weeks in the presence of 30 ng ml^{-1} of anti-CD3 (OKT-3; Miltenyi Biotec). Restimulation with different fungal lysates was performed as described above. To calculate the frequencies of reactive T cells, the mean values were calculated for each antigen and divided by the number of input wells.

Cytotoxicity assay

Cytotoxicity of yeast-reactive CD4$^+$ T cells against adherent small IECs (PELOBiotech) was measured in duplicate by a Real Time Cell Analyzer (RTCA, X-Celligence, ACEA)[55]. By using RTCA, the impedance of the cells is monitored via electronic sensors located on the bottom of a 96-well micro-E-plate. Impedance of the cells reflects changes in cellular parameters such as cell proliferation, morphological changes (for example, spreading, adherence) and cell death, and is expressed as an arbitrary unit called the cell index (CI).

A total of 7,500 adherent IECs cells per well were added to a 96-well micro-E-plate to monitor the impedance of the cells every 3 min for 60 h. As the initial adherence in different wells can differ slightly, the CI was normalized to 1 after having reached the linear growth phase. After 24 h, freshly purified *S. cerevisiae*- and *M. restricta*-reactive CD154$^+$CD69$^+$ T_{mem} cells were added at different effector-to-target

ratios (1:1, 1:2, 1:4). T cells and IECs were cross-linked by the addition of 1 µg ml^{-1} of SEB. T cell-induced lysis of IECs is indicated by the loss of impedance, that is, a decrease in the normalized CI. As a positive control, IECs were treated with 1% Triton X-100 (final concentration). For analysis with RTCA software (v.2.0.0.1301, ACEA), the mean of Triton X-100 samples was calculated and defined as 100% lysis after the addition of effector cells. The percentage of lysis for each sample was calculated in relation to a control sample without effector cells.

Orthotopic TCR replacement in primary human CD4$^+$ T cells

DNA templates (Supplementary Table 1) were designed in silico based on the previously published method[42] and were synthesized by Twist Biosciences in pTwist Amp vectors. Briefly, the constructs comprise the full length of the α- and β-chains of the inserting TCRs flanked by left and right homology arms and contain self-cleaving peptides (P2A and T2A) to provide separation, as well as a poly(A) tail (bGHpA). The β-chain consists of the human variable region and the murine constant region, which is used as a tracking marker.

TCR replacement was performed as previously described[42]. In brief, CD4$^+$ T cells were isolated by negative magnetic selection (CD4$^+$ T Cell Isolation Kit; Miltenyi Biotec). Then, 4×10^7 CD4$^+$ cells were plated on 6-well cell-culture plates in expansion medium, containing TexMACS medium, supplemented with 5% (v/v) human AB-serum, 200 U ml^{-1} of IL-2 and 100 IU ml^{-1} of penicillin, 100 µg ml^{-1} of streptomycin and 0.25 µg ml^{-1} of amphotericin B. CD4$^+$ T cells were subsequently activated for 2 d using the T Cell Activation/Expansion Kit (Miltenyi Biotec). Activated CD4$^+$ T cells were harvested and the activation beads were removed using a MACSiMAG Separator (Miltenyi Biotec). For each nucleofection, 1×10^6 cells were used and mixed with 20 µM ribonucleoprotein (RNP) mixtures (Integrated DNA Technologies (IDT)) and a homology-directed repair template (1 µg) (Twist Biosciences). The RNPs (all components from IDT) were generated in two sequential steps: first, the guide RNAs (gRNAs) were prepared by mixing equal volumes of *trans*-activating CRISPR (tracr)RNA (80 µM stock) with hTRAC CRISPR (cr)RNA (80 µM stock) (crRNA sequences for gRNAs were 5′-GGAGAATGACGAGTGGACCC-3′ for TRBC32, targeting both TRBC1 and TRBC2, and 5′-AGAGTCTCTCAGCTGGTACA-3′ for TRAC) and heating at 95 °C for 5 min, followed by cooling to room temperature (RT). In the second step, gRNAs were assembled with Cas9 nuclease by mixing equal volumes of Cas9 nuclease (6 µM) and gRNA (40 µM) and incubated at RT for 15 min. An electroporation enhancer was added (400 µM stock) to the RNP mixtures. The P3 Primary Cell 4D-Nucleofector X Kit S (Lonza) and a 4D-Nucleofector X unit (Lonza) with the EH100 program were used. Electroporated cells were immediately transferred to 96-well cell-culture plates in expansion medium and were incubated for 5 d at 37 °C and 5% CO_2. After 5 d, TCR-transgenic CD4$^+$ T cells were sorted with FACS on a FACS Aria Fusion (BD Bioscience) based on their mouse TCR-β expression and were further expanded for 2–3 weeks in the presence of 2×10^5 irradiated allogeneic feeder cells until subsequent functional assays were performed. For FACS, cells were stained with fluorochrome-conjugated antibodies to CD4-Vioblue, CD8-PerCP, CD14-PerCP, CD20-PerCP (all Miltenyi Biotec) and mouse TCR-β chain-APC, as well as human TCR-α/β chain-FITC (both BioLegend). After sorting, knocked-in cells were expanded for 2 weeks.

ScRNA-seq assay (10× Genomics)

For scRNA-seq and TCR-seq, yeast-reactive IL-17A producers, IFN-γ producers and double-negative CD154$^+$ T_{mem} cells were sorted with FACS and labeled with barcoded antibodies (CITE-seq). In brief, PBMCs were stimulated with *C. albicans*, *C. tropicalis* and *S. cerevisiae* for 6 h in the presence of 1 µg ml^{-1} of CD40 and 1 µg ml^{-1} of CD28 pure antibody. Cells were labeled with IFN-γ and IL-17A catch reagent (cytokine secretion assay, both Miltenyi Biotec) and incubated for an additional 45 min in RMPI-1640 medium supplemented with 2% (v/v) human AB-serum under continuous rotation. Cells were further labeled with CD154-PE, IL-17A-APC and IFN-γ-FITC, followed by anti-PE MicroBeads, and magnetically enriched by MS Columns (all from Miltenyi Biotec).

Cells were sorted into precoated, low-bind collection tubes, containing sterile, filtered 1× PBS supplemented with 0.5% (v/v) human AB-serum. After sorting, cells were re-added to MS Columns to avoid cell loss during washing steps and stained on the column with 1 µl of hashtag antibodies (TotalSeq-C0251 anti-human hashtag 1 (LNH-94, 1:50), TotalSeq-C0252 anti-human hashtag 2 (LNH-94, 1:50) and TotalSeq-C0253 anti-human hashtag 3 (LNH-94, 1:50) in the presence of Human TruStain FcX in titer 1:20) (all BioLegend) in 50 µl of staining volume. Columns were washed twice and cells were eluted with 500 µl of sterile filtered 1× PBS supplemented with 0.5% (v/v) human AB-serum. Directly before loading, IL-17A$^+$, IFN-γ and CD154$^+$ populations for each antigen were combined, centrifuged, and loaded on a Chromium Next GEM Chip K (10× Genomics) according to the manufacturer's instructions for processing with the Chromium Next GEM Single Cell 5′ Kit v.2. Between 5,000 and 12,000 cells were loaded for each reaction. TCR single-cell libraries were subsequently prepared from the same cells with the Chromium Single Cell V(D)J Enrichment Kit, Human T Cell (10× Genomics). Libraries were sequenced on an Illumina NovaSeq 6000 machine with 2× 100 bp for gene expression and TCR libraries, aiming for 50,000 reads per cell and 5,000 reads per cell, respectively.

Single-cell transcriptome data analysis

The 10× sequencing data were processed using the 10× Genomics Cell Ranger v.6.0.0 software pipeline as previously described[56]. Cellranger mkfastq was used to demultiplex cellular barcodes and produce fastq files and cellranger count was used to map reads to the human genome (GRch38) with STAR aligner[57] and obtain a matrix of transcript counts by cells.

The data analysis was performed with the scanpy Python package v.1.9.0, using Python v.3.7 (ref. 58). As part of the quality control, cells were subjected to the following criteria: (1) >500 expressed genes, (2) >1,000 total unique molecular identifier counts, (3) no doublets based on hashtag antibodies and (4) <5% of mitochondrial RNA. Out of the initial 63,732 cells, 60,130 satisfied these criteria and were used in the subsequent analysis.

The data normalization step included library size normalization to 10,000 counts per cell and $\log_2$(transformation) of the expression data. Highly variable genes were identified and used to reduce the dimensionality of the data to 30 principal components (PCs) with the principal component analysis algorithm. The PC values were adjusted using the harmony algorithm[59] as implemented in scanpy.external.pp.harmony_integrate function to correct the batch effect introduced by differences in sample preparation. Unsupervised clustering of the cells was performed with the Leiden clustering algorithm (scanpy.tl.leiden) and cell subtypes were assigned to the clusters based on the differentially expressed marker genes.

ScTCR repertoire data analysis

Cellranger vdj pipeline was used for V(D)J genes calling from scTCR-seq data. Scirpy Python package v.0.12.0 was used[60] to integrate TCR data with the transcriptomic data, and TCR characteristics were inferred for each cell and defined the clonotypes. Cells were considered to belong to the same clonotype if they had the same TCR-β amino-acid sequence. As a quantitative measure of the clonality of TCR repertoires we calculated Gini's coefficient[61]. Gini's coefficient ranges from 0 to 1, with 0 corresponding to equal abundance of all clonotypes and values close to 1 representing total inequality (that is, high prevalence of one sequence). For Gini's coefficient analysis, samples were normalized by random selection of 500 cells from each individual per fungal antigen to remove the impact of different sample sizes (number of cells per sample). TCR-sharing networks were created and visualized using the Cytoscape software v.3.9.1 (ref. 62). Clonotypes found in one cell only were excluded for network analyses.

Trajectory inference
Pseudotime trajectory analysis was performed using the Monocle v.2 algorithm[35]. Samples were normalized by random selection of 500 cells from each individual per fungal antigen to remove the impact of different sample sizes (number of cells per sample) and the analysis restricted to the gene set of 36 markers (Extended Data Table 3).

Statistical analysis
Statistical parameters including the exact value of *n*, the definition of center, dispersion and precision measure, and statistical significance are reported in the figures and figure legends. Statistical tests were performed with GraphPad Prism software v.9.4.1. Statistical tests were selected based on appropriate assumptions with respect to data distribution and variance characteristics; $P < 0.05$ was considered statistically significant.

Software
Flow-cytometry data were analyzed using FlowJo v.10.9.0 (Tree Star) and Miltenyi MACSquantify v.2.13 (Miltenyi Biotec) software. Graphics and statistics were created with GraphPad Prism software v.9.4.1. TCR-sharing networks were created and visualized with Cytoscape software v.3.9.1 (ref. 62).

Reporting summary
Further information on research design is available in the Nature Portfolio Reporting Summary linked to this article.

Data availability
Raw, paired-end, scRNA-seq fastq files from both gene expression and TCR libraries, as well as processed gene expression and TCR data as feature-barcode matrix files and clonotype tables, respectively, have been deposited at the Gene Expression Omnibus (accession no GSE227638) and GitHub under https://github.com/agbacher/fungi. All other data are available in pseudonymized form within 4 weeks upon request to the corresponding author.

Code availability
All code is deposited in GitHub under https://github.com/agbacher/fungi.

References

52. Bacher, P. et al. Regulatory T cell specificity directs tolerance versus allergy against aeroantigens in humans. *Cell* **167**, 1067–1078.e1016 (2016).
53. Bacher, P. et al. Low-avidity CD4$^+$ T cell responses to SARS-CoV-2 in unexposed individuals and humans with severe COVID-19. *Immunity* **53**, 1258–1271.e1255 (2020).
54. Saggau, C. et al. The pre-exposure SARS-CoV-2-specific T cell repertoire determines the quality of the immune response to vaccination. *Immunity* **55**, 1924–1939.e1925 (2022).
55. Oberg, H. H. et al. Novel bispecific antibodies increase gammadelta T-cell cytotoxicity against pancreatic cancer cells. *Cancer Res.* **74**, 1349–1360 (2014).
56. Zheng, G. X. et al. Massively parallel digital transcriptional profiling of single cells. *Nat. Commun.* **8**, 14049 (2017).
57. Dobin, A. et al. STAR: ultrafast universal RNA-seq aligner. *Bioinformatics* **29**, 15–21 (2013).
58. Wolf, F. A., Angerer, P. & Theis, F. J. SCANPY: large-scale single-cell gene expression data analysis. *Genome Biol.* **19**, 15 (2018).
59. Korsunsky, I. et al. Fast, sensitive and accurate integration of single-cell data with Harmony. *Nat. Methods* **16**, 1289–1296 (2019).
60. Sturm, G. et al. Scirpy: a Scanpy extension for analyzing single-cell T-cell receptor-sequencing data. *Bioinformatics* **36**, 4817–4818 (2020).
61. Sadras, V. & Bongiovanni, R. Use of Lorenz curves and Gini coefficients to assess yield inequality within paddocks. *Field Crops Res.* **90**, 303–310 (2004).
62. Shannon, P. et al. Cytoscape: a software environment for integrated models of biomolecular interaction networks. *Genome Res.* **13**, 2498–2504 (2003).

Acknowledgements
We thank N. Bekel, S. Meise and B. Messner for technical assistance, M. Goldmann and A. Bittroff-Leben for help with generating microbial lysates, A. Gollmer from the popgen biobank for help with recruiting study participants, K. Schober and E.-M. Schuster for help with designing the TCR constructs, and the Flow Cytometry Facility Kiel and the Competence Centre for Genomic Analysis Kiel for support with cell sorting and single-cell sequencing. This research was supported by the German Research Foundation (Deutsche Forschungsgemeinschaft (DFG)) under Germany's Excellence Strategy: EXC2167-Project ID 390884018 'Precision Medicine in Chronic Inflammation' (to W.L., J.R., K.A., A.F., A.S., S. Schreiber and P.B.) and EXC 2051-Project ID 467 390713860 'Balance of the Microverse' (to A.A.B. and B.H.), the RU5042-miTarget (to J.R., K.A., A.F. and P.B.), DFG grant no. 433038070 (to A.F., A.S. and P.B.), DFG grant no. 387835892 (to A.S.), TRR241 Project ID 375876048 (to B.S., A.S. and P.B.), the US National Institutes of Health (grant nos. R01DK121977 and R01AI163007) and a Leona M. and Harry B. Helmsley Charitable Trust grant (to I.D.I.). This project received funding from the European Union (European Research Council (ERC) starting grant 2021, no. 101040023 'MicroT' to P.B.). Views and opinions expressed are, however, those of the author(s) only and do not necessarily reflect those of the European Union or the ERC Executive Agency. Neither the European Union nor the granting authority can be held responsible for them.

Author contributions
G.R.M. and P.B. conceived the project. G.R.M., C.S., P.H., S. Schneiders, A.K.K. and M.B.D. did the investigations. G.R.M., E.T., E.R. and M.B.D. carried out the formal analysis. L.K.S., F.T., M.L., A.B., S.H., S.N., J.K., A.M., G.J., W.L., B. Seegers, H.H., K.A. and S. Schreiber recruited patients and provided clinical data. J.M., B. Siegmund, H.O., D.W., S. Bereswill, M.M.H., J.R., O.K., A.A.B., S. Brunke, B.H. and A.F. provided the resources. P.B. wrote the original draft of the manuscript. P.B., A.S., I.D.I. and S. Schreiber reviewed and edited the manuscript. P.B. supervised the project. All authors provided discussion, participated in revising the manuscript and agreed to the final version.

Funding
Open access funding provided by Christian-Albrechts-Universität zu Kiel.

Competing interests
Since January 2023, E.R. has been an employee of GlaxoSmithKline. The remaining authors declare no competing interests.

Additional information
Extended data is available for this paper at https://doi.org/10.1038/s41591-023-02556-5.

Supplementary information The online version contains supplementary material available at https://doi.org/10.1038/s41591-023-02556-5.

Correspondence and requests for materials should be addressed to Petra Bacher.

Peer review information *Nature Medicine* thanks Kenya Honda, Daniel Mucida and the other, anonymous, reviewer(s) for their contribution to the peer review of this work. Primary Handling Editors: Ulrike Harjes and Saheli Sadanand, in collaboration with the *Nature Medicine* team.

https://doi.org/10.1038/s41591-023-02556-5

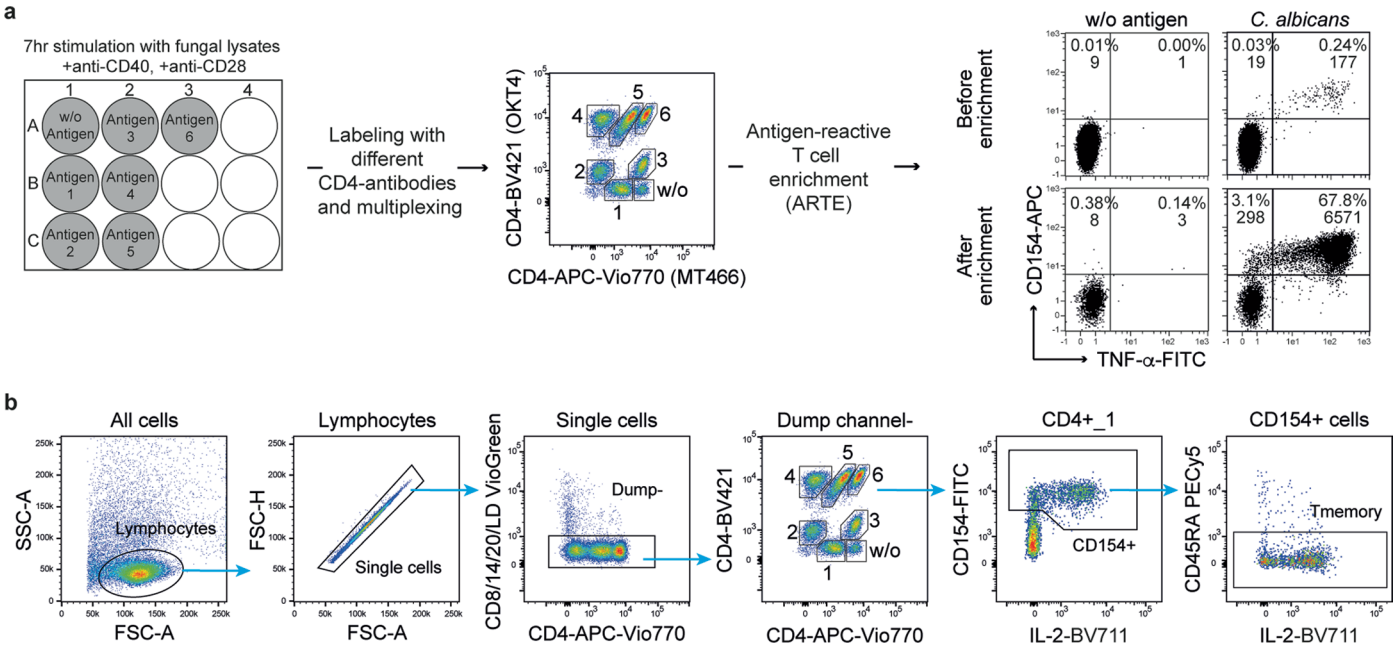

Extended Data Fig. 1 | Antigen-reactive T cell enrichment (ARTE). (**a**) Experimental set-up of ARTE in combination with multiplexing of differently stimulated samples. PBMCs were stimulated with different microbial lysates for 7 hours. Cells were labeled with a CD4-antibody-based fluorescent barcode using different anti-CD4 clones and mixed. Reactive CD154+ T cells were enriched by ARTE. Dot plot examples show *C. albicans* lysate-stimulated cells before enrichment and after magnetic CD154+ enrichment from 2x10e7 PBMCs. Percentage of CD154+ cells within CD4+ T cells and absolute cell counts are indicated. (**b**) Gating strategy following enrichment of CD154+ cells via ARTE.

https://doi.org/10.1038/s41591-023-02556-5

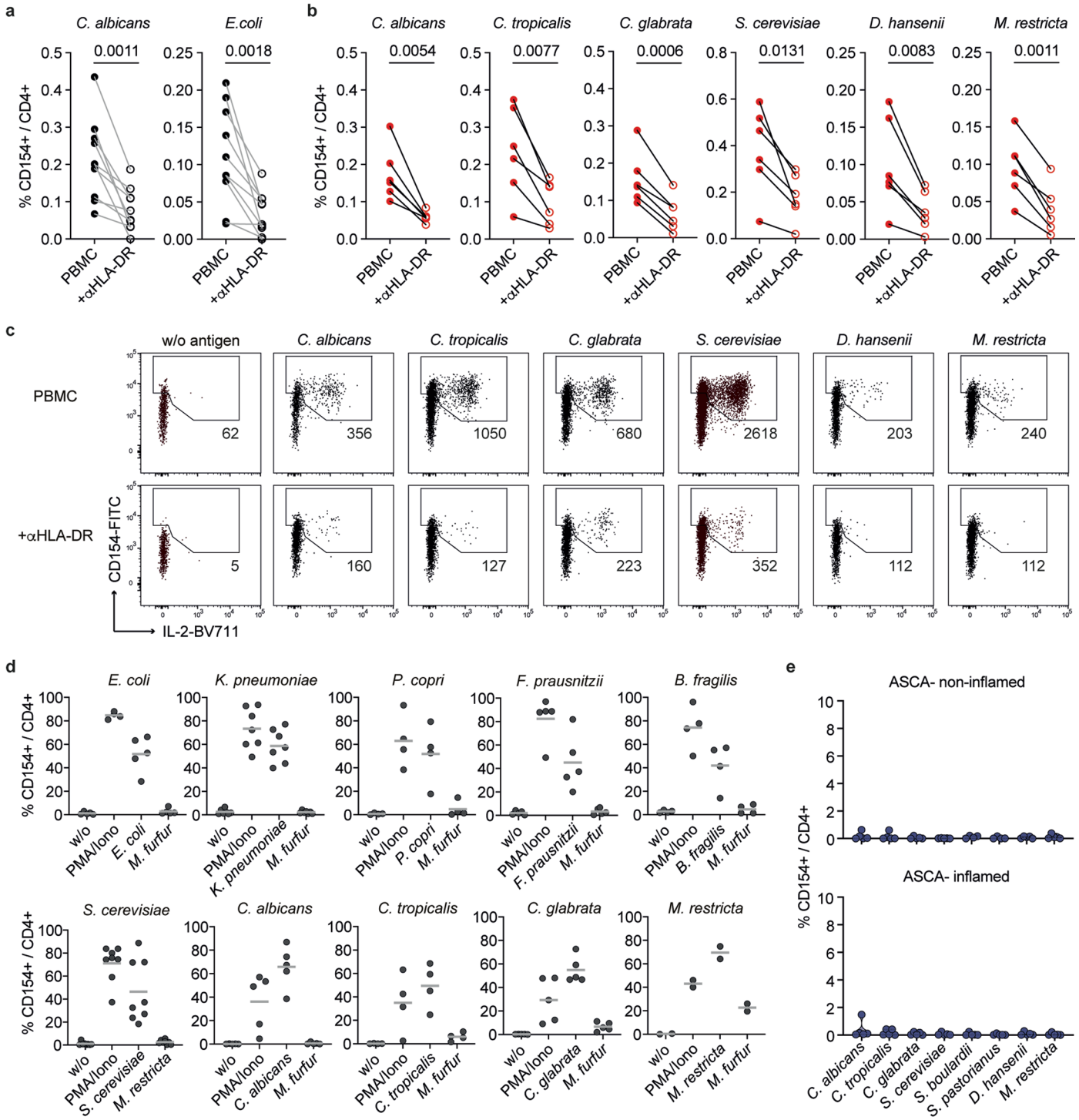

Extended Data Fig. 2 | Specificity of microbial lysate induced CD154 expression. (**a**, **b**) Frequencies of microbial lysate stimulated CD154+ T cells stimulated in presence or absence of an anti-HLA-DR antibody of (**a**) healthy donors (n = 10) and (**b**) CD patients (n = 6). (**c**) Representative flow plots showing CD154 induction in presence or absence of an anti-HLA-DR antibody. Numbers of enriched CD154+ cells are indicated. (**d**) Following stimulation with microbial lysates, CD154+ cells were FACS-purified, expanded for several weeks and restimulated with the specific or unrelated microbial lysates in the presence of autologous antigen presenting cells. PMA-Ionomycin stimulation was used as positive control. Percentage of CD154+ TNFα+ cells within CD4+ is indicated (*E. coli*, *F. prausnitzii*, *C. albicans*, *C. glabrata* n = 5; *K. pneumoniae* n = 7; *P. copri*, *B. fragilis*, *C. tropicalis* n = 4; *S. cerevisiae* n = 8; *M. restricta* n = 2). (**e**) Total CD4+ memory T cells were isolated from biopsies of inflamed and uninflamed intestinal tissue of ASCA- CD patients (n = 5). Cells were seeded at 200 cells/well in multiple wells, expanded and re-stimulated with fungal lysates in presence of autologous APCs. Mean frequencies of reactive CD154+ cells for all wells per patient are shown. Each symbol in (**a**, **b**, **d**, **e**) represents one individual donor. Truncated violin plots with quartiles and range are shown in (**e**). Statistical differences: two-tailed paired t test in (**a**, **b**).

https://doi.org/10.1038/s41591-023-02556-5

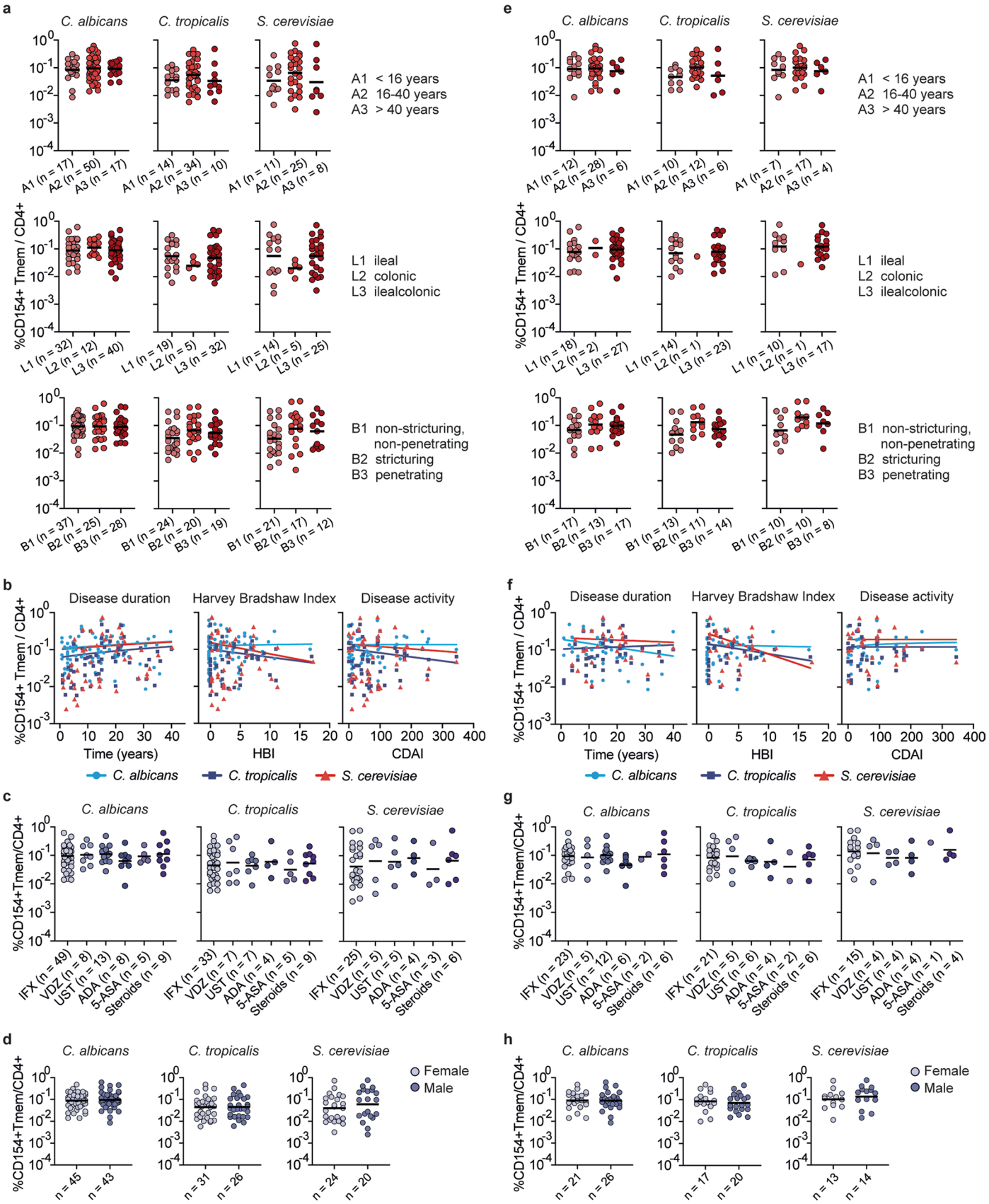

Extended Data Fig. 3 | See next page for caption.

https://doi.org/10.1038/s41591-023-02556-5

Extended Data Fig. 3 | Correlation of T cell data with clinical parameters. Reactive CD4+ T cell frequencies against *C. albicans*, *C. tropicalis* and *S. cerevisiae* were correlated to different clinical parameters in all CD patients (**a**-**d**) or ASCA+ CD patients (**e**-**h**). (**a**, **e**) Influence of age at diagnosis, disease localization or behavior, based on Montreal classification, on fungus-reactive T cell frequencies. n indicates the number of individual donors specified below each group. (**b**, **f**) Spearman correlation of yeast-reactive CD4+ T cell frequencies with disease duration or activity, as determined by Harvey-Bradshaw Index (HBI) or Crohn's disease activity index (CDAI). (**b**, *C. albicans* n = 88, *C. tropicalis* n = 59, *S. cerevisiae* n = 44; **f**, *C. albicans* n = 50, *C. tropicalis* n = 38, *S. cerevisiae* n = 28). (**c**, **g**) Yeast-reactive T cell frequencies according to different treatments. IFX, Infliximab; VDZ, Vedolizumab; UST, Ustekinumab; ADA, Adalimumab; 5-ASA, 5-aminosalicylic acid. n indicates the number of individual donors specified below each group. (**d**, **h**) Yeast-reactive T cell frequencies according to sex. n indicates the number of individual donors specified below each group. Each symbol in **a**-**h** represents one individual donor. Horizontal lines indicate geometric mean values in (**a**, **c**, **d**, **e**, **g**, **h**).

https://doi.org/10.1038/s41591-023-02556-5

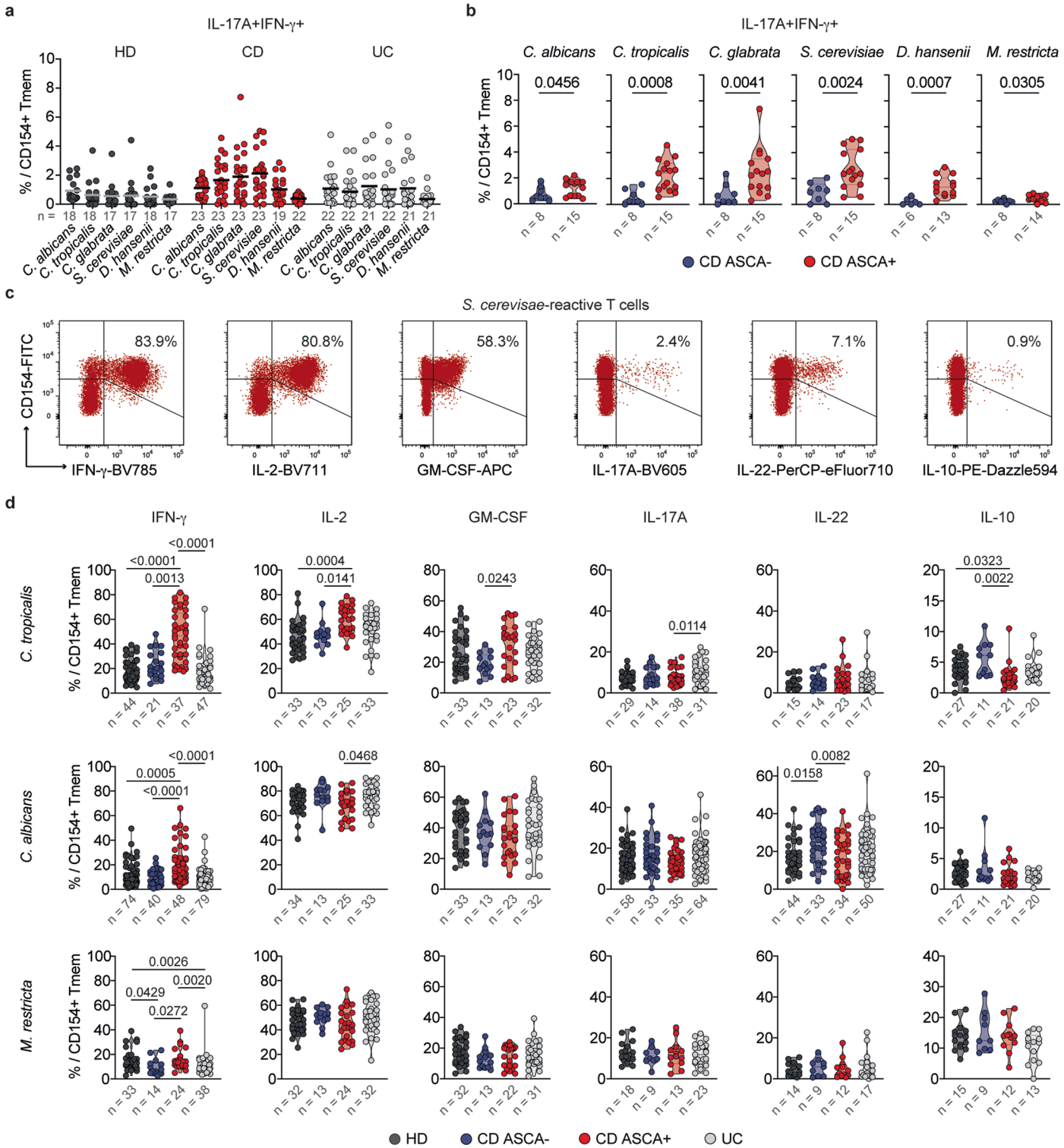

Extended Data Fig. 4 | Cytokine production of yeast-reactive CD4+ T cells. (**a**) Proportion of IL-17A+IFN-γ+ cells reactive against the different fungal antigens. n indicates the number of individual donors specified below each group. (**b**) Proportion of IL-17A+IFN-γ+ cells in CD patients according to their ASCA status. n indicates the number of individual donors specified below each group. (**c**) Example plots for ex vivo cytokine production of *S. cerevisiae*-reactive Tmem following ARTE. Percentages of cytokine positive cells within CD154+ Tmem are indicated. (**d**) Cytokine production of *C. tropicalis, C. albicans* and *M. restricta*-reactive T cells in healthy donors and IBD patients. n indicates the number of individual donors specified below each group. Each symbol in (**a**, **b**, **d**) represents one individual donor, truncated violin plots with quartiles and range are shown in (**b**, **d**). Statistical differences: two-tailed Mann-Whitney test in (**b**); Kruskal-Wallis test with Dunn's post hoc test in (**d**), only significant differences are shown.

https://doi.org/10.1038/s41591-023-02556-5

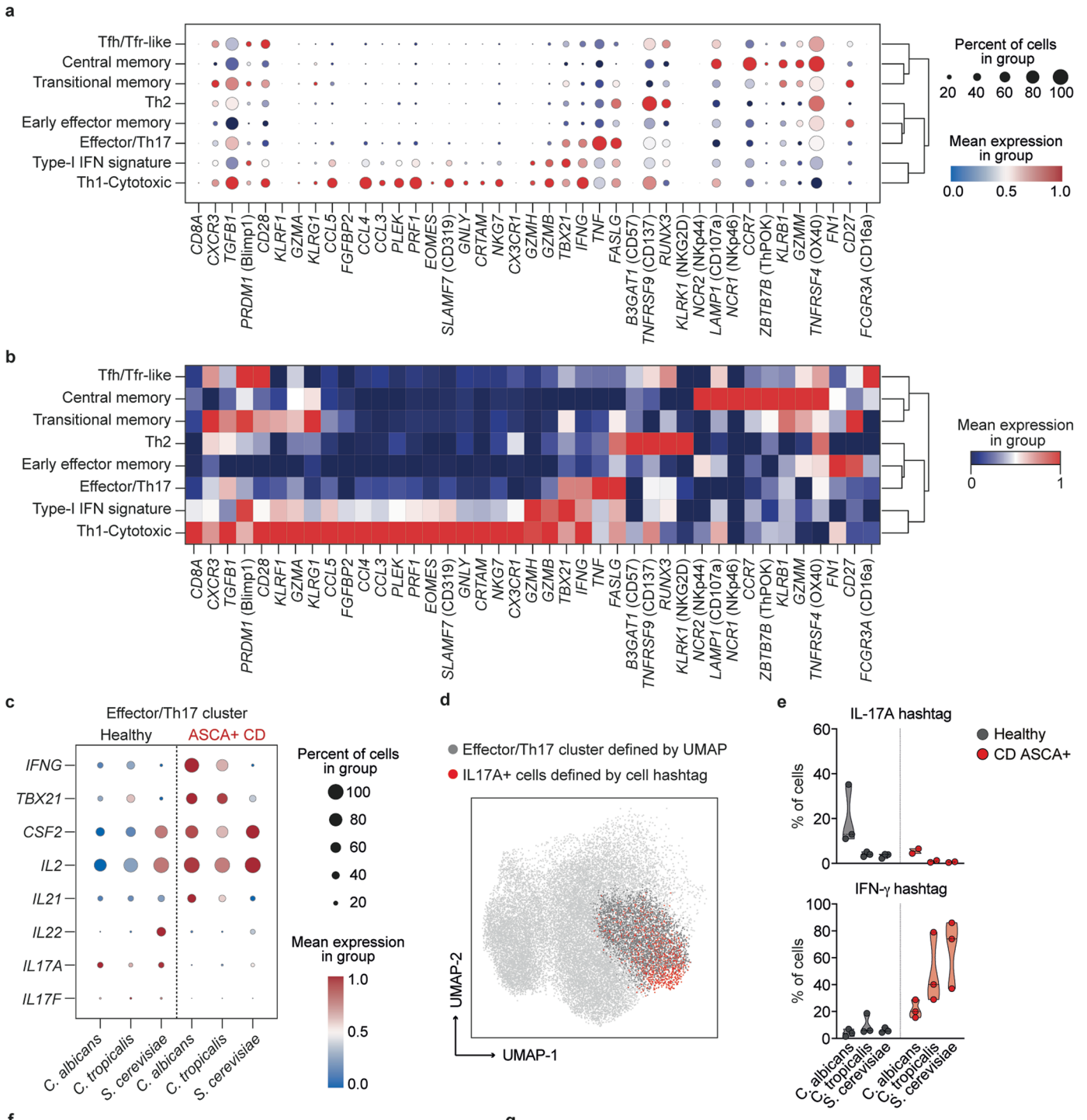

Extended Data Fig. 5 | See next page for caption.

https://doi.org/10.1038/s41591-023-02556-5

Extended Data Fig. 5 | Yeast-responsive Th1 cells express several cytotoxicity-associated markers. (**a**) Dot plot visualization showing the expression of cytotoxicity-associated[32] genes in each T cell cluster. Colors represent the normalized mean expression, and size indicates the proportion of cells expressing the respective genes. (**b**) Heatmap showing the expression of selected genes in each T cell cluster. Colors represent the Z-score-normalized expression amounts. (**c**) Dot plot visualization showing the expression of selected marker genes within the effector/Th17 cluster for healthy donors and CD patients according to antigen specificity. Colors represent the normalized mean expression levels, and size indicates the proportion of cells expressing the respective genes. (**d**) IL-17A producing cells were labeled with hashtag antibodies prior to scRNA sequencing (see Methods) and are plotted as overlay with the effector/Th17 cluster. These data show that only a subset of cells within this cluster has a Th17 signature. (**e**) Proportion of IFN-γ+ or IL-17A+ cells labeled with hashtag antibodies for individual donors and specificities (healthy n = 3, CD n = 3). (**f**, **g**) Expression of cytotoxic markers in (**f**) *C. tropicalis* and (**g**) *C. albicans*-reactive T cells of CD patients according to their ASCA status. (ASCA- n = 8; ASCA+ n = 14). Each symbol in (**f, g**) represents one individual donor. Truncated violin plots with quartiles and range are shown in (**f**, **g**). Statistical differences: Two-tailed Mann-Whitney test in (**f, g**).

https://doi.org/10.1038/s41591-023-02556-5

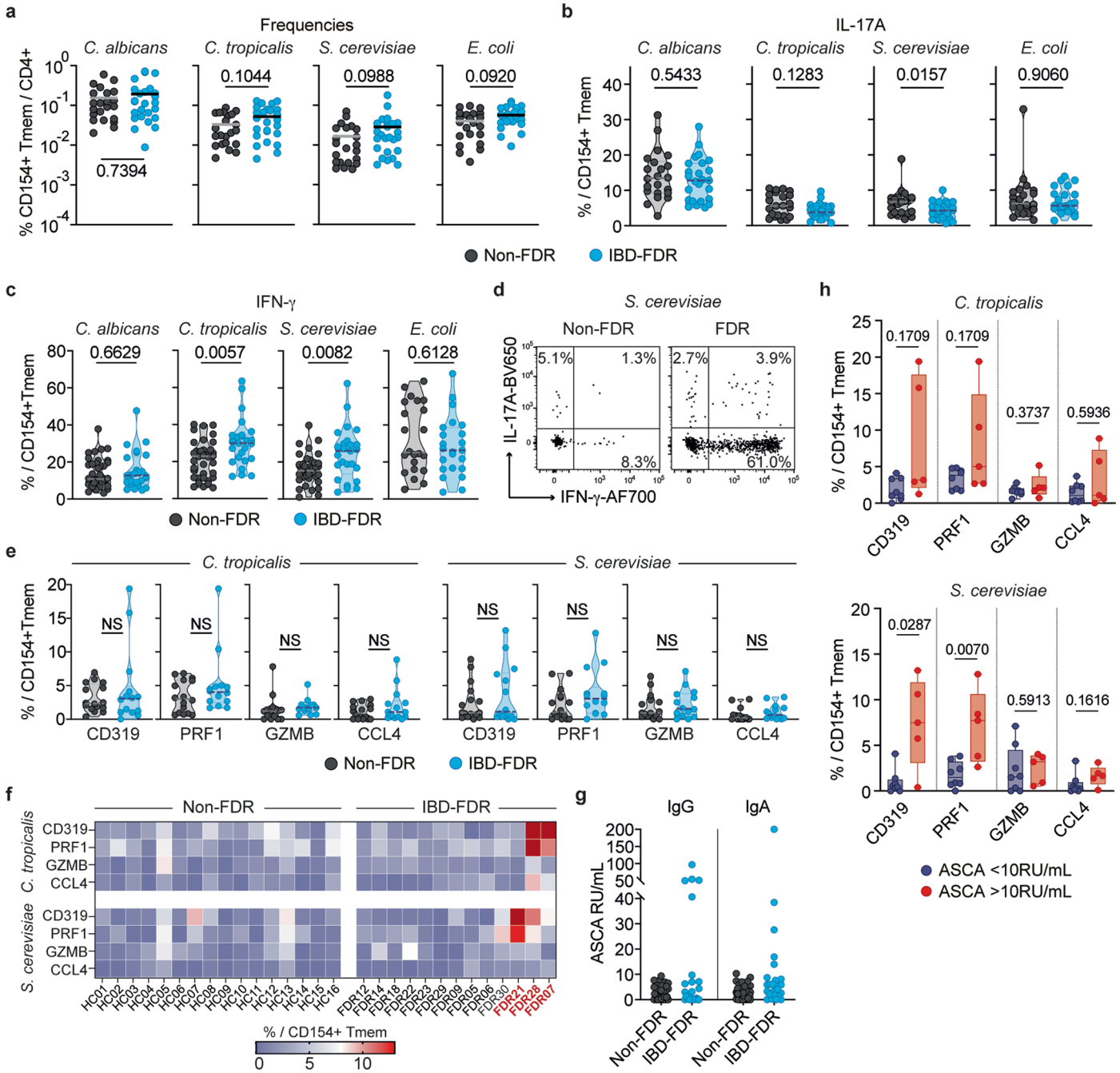

Extended Data Fig. 6 | Alterations of yeast-reactive CD4+ T cells are present in first-degree-relatives of IBD patients (IBD-FDR). (**a**) Frequencies and (**b**) IL-17A production of yeast-reactive T cells in IBD-FDRs (n = 25) and non-FDR controls (n = 22). (**c**) IFN-γ staining of yeast-reactive T cells in IBD-FDRs (n = 25) and non-FDR healthy controls (n = 38). (**d**) Dot plot examples for IFN-γ staining of *S. cerevisiae*-reactive T cells. (**e**) Cytotoxic marker expression of *C. tropicalis* and *S. cerevisiae*-reactive CD154+ Tmem (non-FDR n = 16, IBD-FDR n = 14). (**f**) Heatmap depicting *ex vivo* cytotoxic markers production of yeast-reactive T cells within CD154+ Tmem measured by flow cytometry. (**g**) Serum anti-IgG and IgA ASCA antibody concentrations in non-FDRs (n = 46) and IBD-FDRs (n = 25). (**h**) Cytotoxic marker expression in IBD-FDRs in relation to elevated ASCA levels of the individual IBD-FDRs (ASCA < 10RU/ml n = 8, ASCA > 10 RU/ml n = 5). Individual donors are shown as dots. Each symbol in (**a**, **b**, **c**, **e**, **g**, **h**) represents one individual donor. Horizontal lines indicate mean values in (**a**). Truncated violin plots with quartiles and range are shown in (**b**, **c**, **e**). Box-and-whisker plots are shown in (**h**) with center lines represent the median, box limits represent 25% (lower) and 75% (upper) quartiles and whiskers represent minimum/maximum. Statistical differences: two-tailed Mann-Whitney test in (**a**, **b**, **c**, **e**, **h**).

https://doi.org/10.1038/s41591-023-02556-5

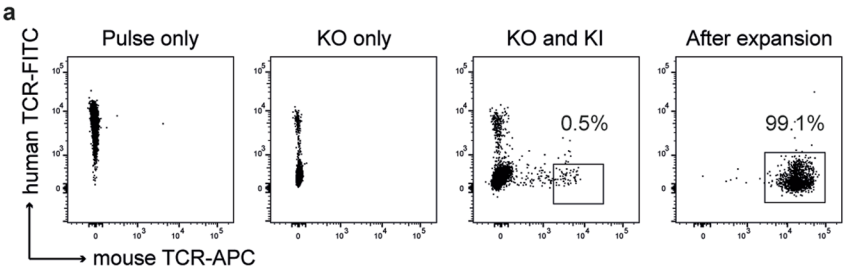

b

TCR	TCR α-chain	TCR β-chain
CD1_TCR7	TGTGCTGTGGACCAGAAAAGCAGCGGAGACAAGCTGACTTTT	TGTGCCACCAGCAGAGAAGGACGGGCAGATACGCAGTATTTT
CD1_TCR4	TGTGCTGTGAGTGAAGGGGACAAACTGGTCTTT	TGCAGTGCTAGAGTTCTAGCGGGAGGTTCCGGGGAGCTGTTTTTT
CD2_TCR5	TGTGCAGCAAGAAAGACTGGGGCAAACAACCTCTTCTTT	TGTGCCAGTAGTATAGGAGTAGCGGGAGGTGAGACCCAGTACTTC
CD2_TCR8	TGTGCAGCAAGTAAGAGCAACTATCAGTTAAT CTGG	TGCAGTGTCCCTAGCGGGGGGGCGGCAGATACGCAGTATTTT
CD2_TCR9	TGTGTGGTGCAACTCACGGGAGGAGGAAACAAACTCACCTTT	TGTGCCAGCAGCCGCACTCGAGCTGGAAACACCATATATTTT
CD3_TCR3	TGTGCTGTGAGTGGGGTTGGAGGCTTCAAAACTATCTTT	TGTGCCAGCAGTGGACCGGGACAGGGGGATCAGCCCCAGCATTTT
CD3_TCR2	TGTGCAATGACCCGTACCGGCACTGCCAGTAAACTCACCTTT	TGTGCCAGCAGCCAAGGTCTGGGACAGGGGCATTCACCCCTCCACTTT

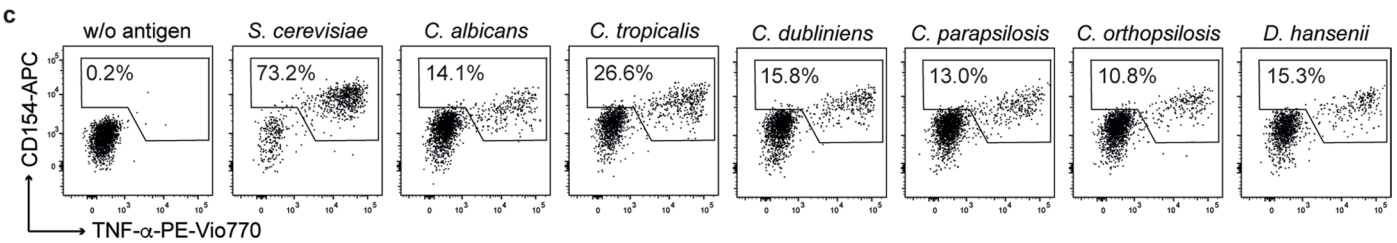

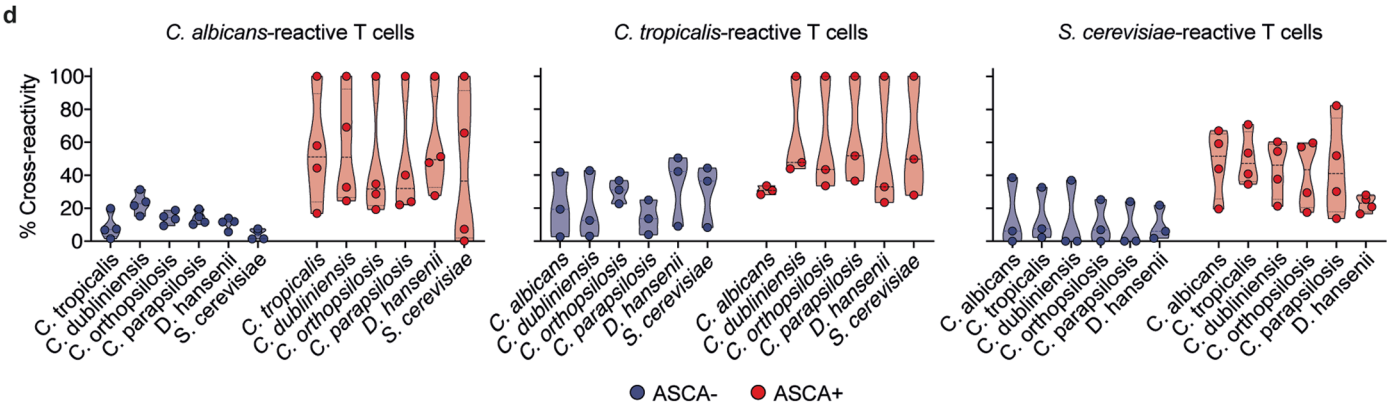

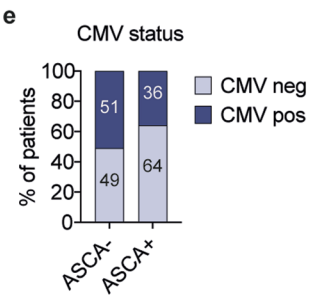

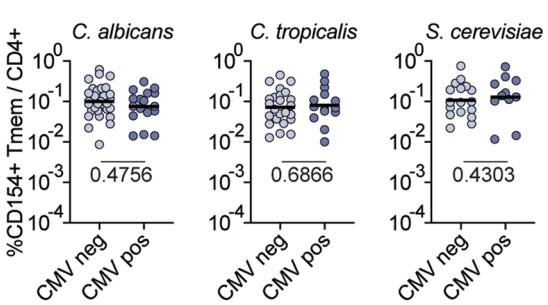

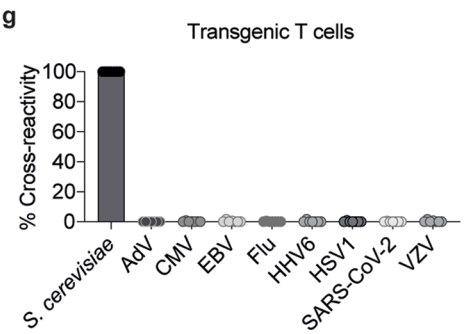

Extended Data Fig. 7 | See next page for caption.

https://doi.org/10.1038/s41591-023-02556-5

Extended Data Fig. 7 | Cross-reactivity of yeast-responsive T cells. (**a**) α/β-TCR constructs of the most expanded cross-reactive TCRs identified from the single cell data set were inserted into primary human CD4+ T cells by orthotopic T cell receptor replacement using CRISPR/Cas. Dot plot examples showing CD4+ T cells with pulse only, knock-out of the endogenous TCR, combined knock-out of the endogenous TCR and knock-in of the transgenic TCR containing a murine β-chain constant region used as tracking marker. Transduced cells were further FACS purified and expanded to high purity. (**b**) TCR-α/β sequences selected from the scRNAseq data set for transgenic T cell generation. (**c**) *S. cerevisiae*-reactive Tmem from an ASCA+ CD patient were expanded and re-stimulated with various yeast species. Percentages of reactive CD154+ TNFα+ cells are indicated. (**d**) Cross-reactivity of expanded yeast-reactive T cells in ASCA- CD patients (*C. albicans* n = 4, *S. cerevisiae*, *C. tropicalis* n = 3) and ASCA+ CD patients (*C. albicans*, *S. cerevisiae* n = 4, *C. tropicalis* n = 3). Cross-reactivity is plotted as percentage in relation to total reactivity after stimulation with the initially used yeast species. (**e**) CMV serum antibody status of ASCA- CD patients (n = 39) and ASCA+ CD patients (n = 49) was determined by ELISA and percentage of CMV negative and CMV positive patients is indicated. (**f**) Yeast-reactive T cell frequencies of ASCA+ patients according to their CMV status (*C. albicans* CMVneg n = 32, CMVpos n = 17; C. tropicalis CMVneg n = 24, CMVpos n = 14; *S. cerevisiae* CMVneg n = 17, CMVpos n = 11). (**g**) TCR transgenic T cells (n = 7) were restimulated with common viral antigens. Cross-reactivity in relation to stimulation with *S. cerevisiae* is shown. Each symbol in (**d**, **f**) represents one individual donor and in (**g**) one TCR transgenic T cell line. Truncated violin plots with quartiles and range are shown in (**d**). Horizontal lines indicate geometric mean values in (**f**). Statistical differences: two-tailed Mann-Whitney test in (**f**).

https://doi.org/10.1038/s41591-023-02556-5

Extended Data Table 1 | Cohort characteristics

	Sample group			
	Healthy	**IBD-FDR**	**UC**	**CD**
Individuals	71	25	79	88
Sex, M/F (N, %)	31/40 (44/56%)	10/15 (40/60%)	41/38 (52/48%)	43/45 (49/51%)
Age (mean±SD, years)	37±13	55±18	42±15	43±14
ASCA IgG positive (N, %)	-	5 (20.0%)	1 (1.3%)	45 (51.1%)
ASCA IgA positive (N, %)	-	3 (12.0%)	1 (1.3%)	46 (52.2%)
ASCA total positive (N, %)	0/0 (0.0%)	5 (20.0%)	2 (2.5%)	49 (55.6%)

https://doi.org/10.1038/s41591-023-02556-5

Extended Data Table 2 | Characteristics of patients with UC and CD

Montreal classification	Ulcerative colitis	Crohn's disease
Age at diagnosis in years		
A1, <16, (N, %)	-	17 (19.3%)
A2, 17-40, (N, %)	-	51 (58.0%)
A3, >40, (N, %)	-	17 (19.3%)
Info not available, (N, %)	-	3 (3.4%)
Location		
L1, ileal, (N, %)	-	30 (34.1%)
L2, colonic, (N, %)	-	15 (17.1%)
L3, ileocolonic, (N, %)	-	39 (44.3%)
Info not available, (N, %)	-	4 (4.5%)
Behaviour		
B1, inflammatory, (N, %)	-	35 (39.8%)
B2, structuring, (N, %)	-	24 (27.3%)
B3, penetrating, (N, %)	-	25 (28.4%)
Info not available, (N, %)	-	4 (4.5%)
Severity		
S0, remission, no symptoms	17 (21.5%)	-
S1, mild symptoms	22 (27.9%)	-
S2, moderate symptoms	15 (19%)	-
S3, severe symptoms	5 (6.3%)	-
Info not available, (N, %)	20 (25.3%)	-
Extensity		
E1, ulcerative colitis	14 (17.7%)	-
E2, left-side UC; distal colitis	24 (30.4%)	-
E3, extensive colitis UC; pancolitis	21 (26.6%)	-
Info not available, (N, %)	20 (25.3%)	-
Disease activity		
HBI, median±IQR	-	2 ±5
Not active 0≤HBI≤4, (N, %)	-	57 (64.8%)
Mild activity, 5≤HBI≤7, (N, %)	-	16 (18.2%)
Moderate activity, 8≤HBI≤16, (N, %)	-	5 (5.7%)
Severe activity, 16≤HBI≤∞, (N, %)	-	1 (1.1%)
pMayo score, median±IQR	1±3	-
Remission <2 (N, %)	30 (38%)	-
Mild, 2-4 (N, %)	17 (21.5%)	-
Moderate, 5-7 (N, %)	5 (6.3%)	-
Severe, >7 (N, %)	0	-
Info not available, (N, %)	27 (34.1%)	9 (10.2%)
CDAI, median±IQR	-	60 ±84
CAI, median±IQR	2.5±4	-
CRP, mean±SD	7.7±21.7	5.4 ±8.8
Medication		
Steroids, (N, %)	14 (17.7%)	11 (12.5%)
5-ASA, (N, %)	34 (43%)	11 (12.5%)
Infliximab, (N, %)	39 (49.3%)	52 (59.1%)
Adalimumab, (N, %)	3 (3.8%)	7 (7.9%)
Ustekinumab, (N, %)	3 (3.8%)	15 (17.1%)
Vedolizumab, (N, %)	18 (22.8%)	8 (9.1%)
Golimumab, (N, %)	1 (1.3%)	-
Tofacitinib, (N, %)	1 (1.3%)	-
No biological treatment, (N, %)	12 (15.2%)	4 (4.5%)
Info not available, (N, %)	2 (2.5%)	2 (2.3%)

https://doi.org/10.1038/s41591-023-02556-5

Extended Data Table 3 | Gene set used for pseudotime trajectory analysis

Gene	UMAP population
PRF1	Th1-cytotoxic
GZMB	Th1-cytotoxic
SLAMF7	Th1-cytotoxic
PLEK	Th1-cytotoxic
NKG7	Th1-cytotoxic
CRTAM	Th1-cytotoxic
CCL3	Th1-cytotoxic
CCL4	Th1-cytotoxic
CCL5	Th1-cytotoxic
IFNG	Th1-cytotoxic
TBX21	Th1-cytotoxic
CSF2	Effector/Th17
IL2	Effector/Th17
IL21	Effector/Th17
IL22	Effector/Th17
IL17A	Effector/Th17
CCR7	Tcm-Tem subsets
SELL	Tcm-Tem subsets
CD27	Tcm-Tem subsets
ICOS	Tfh/Tfr-like
PDCD1	Tfh/Tfr-like
CXCR5	Tfh/Tfr-like
POU2AF1	Tfh/Tfr-like
CTLA4	Tfh/Tfr-like
LAG3	Tfh/Tfr-like
IL10	Tfh/Tfr-like
MX1	Type-I IFN signature
MX2	Type-I IFN signature
ISG15	Type-I IFN signature

nature portfolio

Corresponding author(s): Petra Bacher

Last updated by author(s): Aug 17, 2023

Reporting Summary

Nature Portfolio wishes to improve the reproducibility of the work that we publish. This form provides structure for consistency and transparency in reporting. For further information on Nature Portfolio policies, see our Editorial Policies and the Editorial Policy Checklist.

Statistics

For all statistical analyses, confirm that the following items are present in the figure legend, table legend, main text, or Methods section.

n/a	Confirmed
☐	☒ The exact sample size (*n*) for each experimental group/condition, given as a discrete number and unit of measurement
☐	☒ A statement on whether measurements were taken from distinct samples or whether the same sample was measured repeatedly
☐	☒ The statistical test(s) used AND whether they are one- or two-sided *Only common tests should be described solely by name; describe more complex techniques in the Methods section.*
☒	☐ A description of all covariates tested
☐	☒ A description of any assumptions or corrections, such as tests of normality and adjustment for multiple comparisons
☐	☒ A full description of the statistical parameters including central tendency (e.g. means) or other basic estimates (e.g. regression coefficient) AND variation (e.g. standard deviation) or associated estimates of uncertainty (e.g. confidence intervals)
☐	☒ For null hypothesis testing, the test statistic (e.g. *F*, *t*, *r*) with confidence intervals, effect sizes, degrees of freedom and *P* value noted *Give P values as exact values whenever suitable.*
☒	☐ For Bayesian analysis, information on the choice of priors and Markov chain Monte Carlo settings
☒	☐ For hierarchical and complex designs, identification of the appropriate level for tests and full reporting of outcomes
☒	☐ Estimates of effect sizes (e.g. Cohen's *d*, Pearson's *r*), indicating how they were calculated

Our web collection on statistics for biologists contains articles on many of the points above.

Software and code

Policy information about availability of computer code

Data collection	Flow Cytometry data was acquired using LSR Fortessa (BD Biosciences) and Miltenyi MACSquantify software v2.13. For in vitro expansion cultures and for sequencing experiments, T cells were sorted using a FACS Aria II (BD Biosciences). Sequencing libraries were sequenced on a NextSeq6000 sequencer (Illumina). For measuring the killing capacities against epithelial cells data was acquired in xCELLigence RTCA Analyzer (Agilent).
Data analysis	Flow Cytometry data was analyzed using FlowJo v 10.9.0. Statistical analysis was performed using GraphPad Prism v9.4.1. Analysis of sequencing data was performed as detailed in the methods section, using the following software packages: Cytoscape 3.9.1 Cell Ranger Version 6.0.0 Python v3.7 Scanpy 1.9.0 Scirpy 0.12.0 Monocle v2 RTCA software v 2.0.0.1301 Single cell analysis code can be found in GitHub under https://github.com/agbacher/fungi.

For manuscripts utilizing custom algorithms or software that are central to the research but not yet described in published literature, software must be made available to editors and reviewers. We strongly encourage code deposition in a community repository (e.g. GitHub). See the Nature Portfolio guidelines for submitting code & software for further information.

Data

Policy information about availability of data

All manuscripts must include a data availability statement. This statement should provide the following information, where applicable:

- Accession codes, unique identifiers, or web links for publicly available datasets
- A description of any restrictions on data availability
- For clinical datasets or third party data, please ensure that the statement adheres to our policy

Raw paired-end scRNASeq fastq files from both gene expression and TCR libraries, as well as processed gene expression and TCR data as feature-barcode matrix files and clonotype tables, respectively, have been deposited at GEO (accession number GSE227638). Custom code to reproduce the single RNA and TCR seq analysis under https://github.com/agbacher/fungi. All other data are available in pseudonymized form upon request to the corresponding author.

Human research participants

Policy information about studies involving human research participants and Sex and Gender in Research.

Reporting on sex and gender	Information on sex of the three cohorts was collected and reported in the Extended data Table 1. Gender information was not collected for any of the cohorts.
Population characteristics	This study involved: 167 IBD patients, 25 First-degree-relatives and 71 healthy donors. Population characteristics are described in Extended data Table 1. 88 Crohn's Disease: age mean 43, Standard deviation +- 14, sex: M/F 43/45 79 Ulcerative Colitis: age mean 42, Standard deviation +- 15, sex: M/F 41/38 25 First-degree-relatives: age mean 55, Standard deviation +-18, sex: M/F 10/15 71 Healthy donors: age mean 37, Standard deviation +- 13, sex: M/F 31/40
Recruitment	Healthy donors were randomly recruited with the exclusion factors that they were not aware of having any gastrointestinal diseases or being first degree relatives of IBD patients. First-degree-relatives of IBD patients were recruited from the Kiel IBD Family Cohort Study, a German-wide cohort of IBD patients and their family members. Inflammatory bowel diseases patients were recruited at the Comprehensive Center for Inflammation Medicine (CCIM) and the Gastroenterology-Hepatology Center Kiel (GHZ-Kiel) based on their disease diagnosis and their willingness to give a sample. The CCIM and GHZ-Kiel doctors recruited patients on their schedule routine consultation, we foresee that based on disease/well-being status of the patient, patients under severe disease activity would not be attending their routine consultation. We do not foresee any other recruitment-biases.
Ethics oversight	-Peripheral EDTA blood samples of healthy donors were obtained from blood bank donors of the Institute for Transfusion Medicine, UKSH Kiel, Germany or from in-house volunteers (ethics committee CAU Kiel D578/18, D427/19). -Peripheral EDTA blood samples from patients with inflammatory bowel diseases were obtained from the Department of Internal Medicine I, UKSH Kiel, the Comprehensive Center for Inflammation Medicine (CCIM) and the Gastroenterology-Hepatology Center Kiel (ethics committee CAU Kiel D427/19). -Biopsies from inflamed and non-inflamed intestinal tissue were collected from CD patients that underwent colonoscopy (ethics committee CAU Kiel under the file: B 231/89-1/13). - First-degree-relatives of IBD patients (IBD-FDRs) were recruited from the Kiel IBD Family Cohort Study, a German-wide cohort of IBD patients and their family members (ethics committee CAU Kiel A117/13), built by the popgen Biobank at Kiel University/University Hospital SH in Kiel.

Note that full information on the approval of the study protocol must also be provided in the manuscript.

Field-specific reporting

Please select the one below that is the best fit for your research. If you are not sure, read the appropriate sections before making your selection.

☒ Life sciences ☐ Behavioural & social sciences ☐ Ecological, evolutionary & environmental sciences

For a reference copy of the document with all sections, see nature.com/documents/nr-reporting-summary-flat.pdf

Life sciences study design

All studies must disclose on these points even when the disclosure is negative.

Sample size	The sample size was sufficient to demonstrate statistically significant differences in comparisons between experimental groups by the appropriate statistical tests. The sample size was also determined to be adequate based on reproducibility between independent experiments.
Data exclusions	No data were excluded from the analysis.

Replication	All of the experiments were successfully replicated, by measuring several individual donors of each cohort on different days in individual experiments. The data set includes a sufficient human sample size, taking into consideration the variability expected when using human samples.
Randomization	IBD patients were allocated into groups based on the disease diagnosis (Ulcerative colitis or Crohn's Disease). First-degree-relatives of IBD patients were allocated into the cohort based on their familial-association with IBD patients. Healthy donors were allocated into their group with the exclusion factors that they were not aware of having any gastrointestinal diseases or being first degree relatives of IBD patients. No additional randomization or group selection was performed.
Blinding	No blinding was performed due to patients being selected on their disease phenotype. First-degree-relatives experiments were not blinded due to selection based on their familial connection to IBD patients. Healthy donors experiments were not blinded due to in-house volunteer manner of collection.

Reporting for specific materials, systems and methods

We require information from authors about some types of materials, experimental systems and methods used in many studies. Here, indicate whether each material, system or method listed is relevant to your study. If you are not sure if a list item applies to your research, read the appropriate section before selecting a response.

Materials & experimental systems

n/a	Involved in the study
☐	☒ Antibodies
☒	☐ Eukaryotic cell lines
☒	☐ Palaeontology and archaeology
☒	☐ Animals and other organisms
☒	☐ Clinical data
☒	☐ Dual use research of concern

Methods

n/a	Involved in the study
☒	☐ ChIP-seq
☐	☒ Flow cytometry
☒	☐ MRI-based neuroimaging

Antibodies

Antibodies used

CD3-PE (clone: REA613) 1:50 - Cat#130-113-139
CD4-APC-Vio770 (clone: M-T466) 1:50 - Cat#130-113-251
CD4-VioBlue (clone: REA623) 1:50 - Cat#130-114-534
CD4-FITC (clone: REA623) 1:50 - Cat#130-114-585
CD8-VioGreen (clone: REA734) 1:50 - Cat#130-110-684
CD8-PerCP (clone: BW135/80) 1:50 - Cat#130-113-160
CD14-VioGreen (clone: REA599) 1:50 - Cat#130-110-525
CD14-PerCP (clone: TÜK4) 1:50 - Cat#130-113-150
CD20-VioGreen (clone: LT20) 1:50 - Cat#130-113-379
CD20-PerCP (clone: LT20) 1:50 - Cat#130-113-376
Viobility 405/520 Fixable Dye (1:100) - Cat#130-110-207
CD45RA-VioGreen (clone: REA562) 1:50 - Cat#130-113-369
CD45RO-APC (clone: REA611) 1:50 - Cat#130-113-369
CD69-PE (clone: REA824) 1:50 - Cat#130-112-613
CD154-FITC (clone: REA238) 1:50 - Cat#130-113-612
CD154-APC (clone: REA238) 1:50 - Cat#130-113-610
TNF-α-PE-Vio770 (clone: cA2) 1:50 - Cat#130-120-492
CD197 (CCR7)-PE-Bio770 (clone: REA108) 1:50 - Cat#130-118-350
IL-17A-PE-Vio770 (clone: REA1063) 1:50 - Cat#130-118-248
IL-21-VioR667 (clone: REA1039) 1:50 - Cat#130-117-423
IL-21-PE (clone: REA1039) 1:50 - Cat#130-117-421
Perforin-PE (clone: REA1061) 1:50 - Cat#130-118-117
GM-CSF-APC (clone: REA1215) 1:50 - Cat#130-123-420
GM-CSF-PE-Vio770 (clone: REA1215) 1:50 - Cat#130-123-422
Integrin b7-PE-Vio770 (REAfinity) 1:50 - Cat#130-106-442
Anti-HLA-DR (clone: AC122) 100ug/mL- Cat#130-108-056
CD154 MicroBeads kit - Cat#130-092-658
CD14 MicroBeads, human - Cat#130-050-201
IL-17 Secretion Assay – Detection Kit - Cat#130-094-536
IFN-γ Secretion Assay – Detection Kit - Cat#130-090-433
CD28 pure – functional grade, human (clone: 15E8) - Cat#130-093-375
CD40 pure – functional grade, human (clone: HB14) - Cat#130-094-133
CD3 pure – functional grade, human (clone: OKT3) - Cat#130-093-387
Anti-HLA-DR (clone: LT43) 100ug/mL- Cat#BE0306
CD4-BV421 (clone: OKT4) 1:20 - Cat#317434
CD45RA-PE-Cy5 (clone: HI100) 1:60 - Cat#304110
IFN-γ-BV785 (clone: 4S.B3) 1:20 - Cat#502542
IL-2-BV605 (clone: MQ1-17H12) 1:20 - Cat#500332

IL-2-BV711 (clone: MQ1-17H12) 1:20 - Cat#500346
IL-10-PE-Dazzle-594 (clone: JES3-9D7) 1:20 - Cat#501426
IL-17A-BV605 (clone: BL168) 1:20 - Cat#512326
Granzyme-B-PerCP-Cy5 (QA16A02) 1:20 - Cat#372212
CD319-PE-Dazzle-594 (clone: 162.1) 1:20 - Cat#331812
TNF-α-BV650 (clone: MAb11) 1:20 - Cat#502938
anti-mouse-TCRb-APC (clone: H57-597) 1:20 - Cat#109212
anti-human-TCRαb-FITC (clone: IP26) 1:20 - Cat#306706
Human TruStain FcX 1:20 - Cat#422302
IL-17A-BV650 (clone: N49-653) 1:20 - Cat#563746
Integrin b7-BV650 (clone: FIB504) 1:20 - Cat#564285
CCL4 (MIP-1b)-AF770-(clone: D21-1351) 1:20 - Cat#561278
Ki-67-AF700 (clone: B56) 1:20 - Cat#561277
Ki-67-R718 (clone: B56) 1:20 - Cat#566963
Ki-67-BV480 (clone: B56) 1:20 - Cat#566172
IL-22-PerCP-eFluor710 (clone: IL22JOP) 1:100 - Cat#46722282
TotalSeq-C0251 anti-human Hashtag 1 (clone: LNH-94) Biolegend Cat#394661 (1:50)
TotalSeq-C0252 anti-human Hashtag 2 (clone: LNH-94) Biolegend Cat#394663 (1:50)
TotalSeq-C0253 anti-human Hashtag 3 (clone: LNH-94) Biolegend Cat#394665 (1:50)

Validation

All antibodies purchased were validated by their manufacturers in-house.
Miltenyi Biotec:
By using the three pillars of antibody validation: 1. Antibody reproducibility and consistency (Pure antibody products and lot-to-lot consistency performance); 2. Antibody specificity (Epitope competition assay, KO validation using targeted genome editing and RNAi knockdown); 3. Antibody sensitivity (Functional testing of every product prior to release, performance comparison & compatibility with fixation).
https://www.miltenyibiotec.com/DE-en/products/macs-antibodies/antibody-validation.html

BioLegend:
Flow cytometry reagents
Specificity testing of 1-3 target cell types with either single- or multi-color analysis (including positive and negative cell types)
Once specificity is confirmed, each new lot must perform with similar intensity to the in-date reference lot. Brightness (MFI) is evaluated from both positive and negative populations.
Each lot product is validated by QC testing with a series of titration dilutions.
TotalSeq™ Antibodies
Bulk lots are tested by PCR and sequencing to confirm the oligonucleotide barcodes. They are also tested by flow cytometry to ensure the antibodies recognize the proper cell populations.
Bottled lots are tested by PCR and sequencing to confirm the oligonucleotide barcodes.
https://www.biolegend.com/en-us/quality/product-development

BD Biosciences:
https://www.bdbiosciences.com/en-de/products/reagents/flow-cytometry-reagents/research-reagents/quality-and-reproducibility
1. Antibody specificity: All flow cytometry reagents are titrated on the relevant positive or negative cells.
2. Quality Control: Quality control testing of new, manufactured lots are performed side-by-side with a previously accepted lot as a control, helping to serve as a reference for comparison and assuring that performance of the new lot is both reliable and consistent.
3. Lot-to-lot consistency: Testing with prior batches as reference helps you obtain consistent results with the new batch relative to the previous batches.

Flow Cytometry

Plots

Confirm that:

☒ The axis labels state the marker and fluorochrome used (e.g. CD4-FITC).

☒ The axis scales are clearly visible. Include numbers along axes only for bottom left plot of group (a 'group' is an analysis of identical markers).

☐ All plots are contour plots with outliers or pseudocolor plots.

☒ A numerical value for number of cells or percentage (with statistics) is provided.

Methodology

Sample preparation

Peripheral blood mononuclear cells (PBMCs) were freshly isolated from EDTA blood on the day of blood donation by density gradient centrifugation (Biocoll, Biochrom, Berlin, Germany). 1-2x10e7 PBMCs were plated in RPMI-1640 medium (GIBCO), supplemented with 5% (v/v) human AB-serum (Sigma Aldrich, Schnelldorf, Germany) in 12-well cell culture plates and stimulated for 7 h in presence of 1 µg/mL CD40 and 1 µg/mL CD28 pure antibody (both Miltenyi Biotec, Bergisch Gladbach, Germany). 1 µg/mL Brefeldin A (Sigma Aldrich) was added for the last 2 h.

Instrument

LSR Fortessa, FACS ARIA II (both BD Biosciences), MAQS-Quant16, MAQS-QuantX (both Miltenyi Biotec), Northern Lights (Cytek Biosciences), xCELLigence RTCA Analyzer (Agilent), 10x Chromium (10X Genomics).

Software

Miltenyi MACSquantify software (v2.13) and FlowJo (v10.9.0.)

Cell population abundance	All experiments include cells that were magnetically enriched following the ARTE protocol as described in the methods. Frequencies of antigen-specific T cells were determined based on the cell count of CD154+ CD4+T cells after enrichment, normalized to the total number of CD4+ T cells applied on the column. For each stimulation, CD154+ background cells enriched from the non-stimulated control were subtracted.
Gating strategy	All recorded events were gated according to FSC and SSC as lymphocytes; single cells were further selected using FSC-H vs. FSC-A. Subsequently living cells were identified as CD8-, CD14- CD20- and Viobility 405/520 Fixable Dye negative gated against CD4-APC-Vio770 (Clone MT466). The differentially stimulated cells were labeled with CD4-antibody-based fluorescent barcodes, allowing multiplexed analysis of T cell reactivity against different species as shown in Figure S1A. Each CD4+ population was then gated on CD154-FITC/IFN-g-BV785 and further gated into CD45RA-PE-Cy5 negative. All phenotypic and functional markers were analyzed withing CD154+CD45RA- cells.

☒ Tick this box to confirm that a figure exemplifying the gating strategy is provided in the Supplementary Information.